# Accepted Manuscript


A few atoms make the difference: synthetic, CD, NMR and computational studies on antiviral and antibacterial activities of glycopeptide antibiotic aglycon derivatives

Ilona Bereczki, Attila Mándi, Erzsébet Rőth, Anikó Borbás, Ádám Fizil, István Komáromi, Attila Sipos, Tibor Kurtán, Gyula Batta, Eszter Ostorházi, Ferenc Rozgonyi, Evelien Vanderlinden, Lieve Naesens, Ferenc Sztaricskai, Pál Herczegh

PII: S0223-5234(15)00124-5

DOI: 10.1016/j.ejmech.2015.02.028

Reference: EJMECH 7710

To appear in: *European Journal of Medicinal Chemistry*

Received Date: 17 December 2014

Revised Date: 17 February 2015

Accepted Date: 19 February 2015

Please cite this article as: I. Bereczki, A. Mándi, E. Rőth, A. Borbás, Á. Fizil, I. Komáromi, A. Sipos, T. Kurtán, G. Batta, E. Ostorházi, F. Rozgonyi, E. Vanderlinden, L. Naesens, F. Sztaricskai, P. Herczegh, A few atoms make the difference: synthetic, CD, NMR and computational studies on antiviral and antibacterial activities of glycopeptide antibiotic aglycon derivatives, *European Journal of Medicinal Chemistry* (2015), doi: 10.1016/j.ejmech.2015.02.028.

# A few atoms make the difference: synthetic, CD, NMR and computational studies on antiviral and antibacterial activities of glycopeptide antibiotic aglycon derivatives

Ilona Bereczki[a], Attila Mándi,[b*] Erzsébet Rőth,[a] Anikó Borbás,[a] Ádám Fizil,[b] István Komáromi,[c] Attila Sipos,[a] Tibor Kurtán,[b] Gyula Batta,[b*] Eszter Ostorházi,[d] Ferenc Rozgonyi,[d] Evelien Vanderlinden,[e] Lieve Naesens,[e*] Ferenc Sztaricskai,[a†] Pál Herczegh[a*]

[a]Department of Pharmaceutical Chemistry, Medical and Health Science Center, University of Debrecen, Egyetem tér 1, H-4010 Debrecen, Hungary,
[b]Department of Organic Chemistry, University of Debrecen, Egyetem tér 1, H-4010 Debrecen, Hungary,
[c]Vascular Biology, Thrombosis and Hemostasis Research Group, Hungarian Academy of Sciences, University of Debrecen, Nagyerdei krt. 98, H-4032 Debrecen, Hungary,
[d]Microbiology Laboratory, Department of Dermatology, Venerology and Dermatooncology, Semmelweis University, Mária u. 41, H-1085 Budapest, Hungary,
[e]Rega Institute for Medical Research, KU Leuven, B-3000 Leuven, Belgium

**Abstract** Despite the close structural similarity between the heptapeptide cores of the glycopeptide antibiotics teicoplanin and ristocetin, synthetically modified derivatives of their aglycons show significantly different antibacterial and antiviral properties.The teicoplanin aglycon derivatives with one exception proved to be potent antibacterials but they did not exhibit anti-influenza virus activity. In contrast, the aglycoristocetin derivatives generally showed high anti-influenza virus activity and possessed moderate antibacterial activity. A systematic structure-activity relationship study has been carried out on ristocetin and teicoplanin aglycon derivatives, to explore which structural differences are responsible for these markedly different biological activities. According to electronic circular dichroism and *in silico* conformational studies, it was found that the differences in anti-influenza virus activity are mainly determined by the conformation of the heptapeptide core of the antibiotics controlled by the presence or absence of chloro substituents. Knowledge of the bioactive conformation will help to design new analogues with improved anti-influenza virus activity. For the teicoplanin derivatives, it was shown that derivatization to improve the antiviral efficacy was accompanied by a significant decrease in antibacterial activity.

**Keywords:** teicoplanin aglycon, ristocetin aglycon, antibacterial, antiviral, conformation

† Deceased on 23/03/2012

*Corresponding authors. Tel.: +36 52 512 900 22895; fax: +36 52 512 914. E-mail address: herczeghp@gmail.com (P. Herczegh); mandi.attila@science.unideb.hu (A. Mándi); batta.gyula@science.unideb.hu (G. Batta); lieve.naesens@rega.kuleuven.be (L. Naesens)
(L. Naesens)

## Introduction

Several years ago, we started a project focussed on semisynthetic investigation of the aglycons of the glycopeptide antibiotics teicoplanin and ristocetin. Inspired by examples of the semisynthetic antibiotics telavancin [1], dalbavancin [2] and oritavancin [3], we initially introduced lipophilic, mainly aromatic, side chains into the ristocetin aglycon molecule [4]. Ristocetin is not applied in medical practice because of its blood platelet aggregating properties [5]. It is known that this side effect can be attributed to the presence of an L-rhamnose moiety in the ristocetin molecule [6]. Therefore, by removing the sugars from ristocetin and reattaching them by click reaction, we obtained new antibacterials devoid of this platelet aggregating activity [7].

A decade ago, Preobrazhenskaya et al. reported on the anti-HIV (and other antiviral) activities of a series of semisynthetic glycopeptide antibiotics bearing preferably lipophilic side chains [8]. We therefore evaluated the antiviral activity of several of our ristocetin derivatives obtained from ristocetin aglycon **1**, by the squaramide coupling reaction with various amines [9]. Some of the new squaramides exhibited pronounced activity against influenza A and B viruses. Among them, the 4-phenylbenzyl substituted derivative **2** proved to be the most potent compound, displaying strong and broad anti-influenza virus activity, [10] and possessing also a moderate antibacterial activity [4] (Figure 1). Detailed mechanistic studies demonstrated that **2** interferes with influenza virus replication by disturbing endocytotic uptake of the virus, resulting in its intracytoplasmic trapping prior to nuclear entry of the viral genome [10].

**Figure 1**. Structures of ristocetin aglycon **1**; its *N*-terminally modified derivative **2** which has potent and broad-activity against influenza virus; teicoplanin aglycon **3**; and teicoplanin pseudoaglycon **4**. The main differences between the glycopeptide cores are highlighted in magenta.

Teicoplanin and ristocetin have nearly the same cross-linked linear heptapeptide aglycon with only a few differences. Teicoplanin aglycon **3** has a free carboxylic group and also two chloro substituents on the aromatic rings. Ristocetin aglycon **1** is a methyl ester and contains no chloro substituents, but has a hydroxylic group in a benzylic position as well as a methyl substituent on one of its aromatic rings (Fig 1). Because of the structural similarities, we decided to perform several chemical transformations both on teicoplanin and ristocetin aglycon derivatives, and studied their antibacterial and antiviral properties. However, while

aglycon **1** could easily be achieved from ristocetin by the Boger's HF-method [11], similar anhydrous hydrogen fluoride treatment of teicoplanin provided pseudoaglycon **4** with a remaining *N*-acetyl glucosamine residue, the removal of which required harsh conditions and proceeded with low yield. Therefore, besides installing lipophilic side chains to the *N*-terminal group of aglycoristocetin, we made similar transformations to teicoplanin pseudoaglycon [12-15]. Surprisingly, despite the close structural resemblance, significantly different antiviral properties were found for the two series of semisynthetic antibiotics. The teicoplanin derivatives did not exhibit anti-influenza virus activity, but most of them proved to be very potent antibacterials with outstanding activities against multidrug-resistant bacteria. In contrast, the aglycoristocetin derivatives generally showed moderate antibacterial activity, but possessed high anti-influenza virus activity.

In the present work, we report on a systematic structure – biological activity relationship study of aglycon derivatives carrying the same 4-phenylbenzyl squaramide moiety as compound **2**. In order to explore or define the structural requirements of the glycopeptide core for the antiviral activity, synthesis and biological evaluation of teicoplanin aglycon and pseudoaglycon derivatives were undertaken using compound **2** as the lead compound. Hence, the easily available teicoplanin pseudoaglycon **4** was modified in successive synthetic steps, involving deglycosylation, methyl ester formation and didechlorination. In this way, we wanted to increase the structural resemblance to the ristocetin aglycon derivative **2**, and study how these modifications affect the antibacterial and anti-influenza virus activities. NMR, CD and computational studies were also performed to provide a rationale for the observed structure-activity trends.

## Results and Discussion

### Synthesis and biological evaluation

First, the 4-phenylbenzyl squaramide moiety was introduced to the *N*-terminus of the peptide core of teicoplanin ψ-aglycon **4** by using the two-step Tietze conjugation method [16]. Condensation of **4** and the squaric acid derivative **5** resulted in **6**, reaction of which with 4-phenylbenzylamine afforded compound **8** in 41% yield over two steps. As ristocetin aglycon exists in methyl ester form, the free *C*-terminus of **4** was esterified with MeOH, and the obtained methyl ester **9** was transformed, through the squaric acid **10**, to another squaramide derivative, compound **11** (Scheme 1). The antibacterial activities were excellent for the pseudoaglycone methyl ester **9** and somewhat lower for its squarate **10** (Table 1). The ester **11** with a lipophilic side chain was very active against vancomycin- and teicoplanin-resistant

strains, while its carboxylic acid analog **8** possessed no activity against enterococci having vanA resistance genes and exhibited weak activity against enterococci with vanB resistance genes. Compounds **8**, **9**, **10** and **11** were completely inactive against influenza virus (Table 2).

**Scheme 1**. Synthesis of **8** and **11** as teicoplanin-pseudoaglycon-counterparts of compound **2**

In order to increase the similarity of the squaramides obtained from teicoplanin to **2**, the *N*-acetyl-D-glucosamine moiety of **4** was removed hydrolytically, and aglycon **3** was transformed to the free carboxylate **13** and methyl ester **15**, according to the squaramide method described above (Scheme 2). Carboxylic acid **13** proved to be a good antibacterial but its methyl ester **15** had no activity. Both of them were inactive against influenza virus. The structural differences between **2** and **15** are: a methyl attached to an aromatic ring and a hydroxyl group in the benzylic position of **2**, and two aromatic chloro substituents in **15**.

**Scheme 2**. Transformation of teicoplanin pseudoaglycon **4** into the *N*-terminally modified teicoplanin aglycon **13** and its methyl ester **15**

**Table 1.** Antibacterial activity of the synthesized compounds

Finally, compound **18**, the closest analog of **2** available from **4**, was prepared via a sequence of reactions (Scheme 3). First, replacement of the chloro substituents by hydrogens was accomplished by catalytic hydrogenation under 4 atm pressure to give **16**. Subsequent hydrolytic removal of *N*-acetylglucosamine followed by esterification at the C-terminus resulted in **17** which was equipped with the 4-phenylbenzyl squaramide moiety to provide **18**.

**Scheme 3**. Transformation of teicoplanin pseudoaglycon **4** into the *N*-terminally modified didechlorinated teicoplanin aglycon methyl ester **18** via didechlorinated teicoplanin aglycon methyl ester **17**

**Table 2.** Activity in influenza virus-infected MDCK[a] cells

Compound **18** exhibited modest antibacterial activity, but displayed high anti-influenza virus activity against both the A/H1N1 and A/H3N2 subtype. It was inactive, however, against influenza B virus.

Summarizing the synthetic results, starting from teicoplanin pseudoaglycon **4**, we changed its structural elements in a stepwise order, to approximate the structure of ristocetin aglycon

derivative **2** which has strong anti-influenza virus activity. The end point of these transformations was compound **18**, the structure of which shows the closest similarity to **2**.

Biological evaluation of the novel derivatives showed that removal of the chloro substituents significantly decreases, if not eliminates, the antibacterial activity. The other synthetic modifications of **4** (i.e. other than didechlorination) only slightly affected the antibacterial activity.

On the other hand, the antiviral evaluations revealed that only the ristocetin derivative **2** and its closest analog **18** possess anti-influenza virus activity. Presence of the chloro substituents proved to be detrimental for the influenza virus inhibitory effect. To explain this finding, we decided to study how these small structural differences can influence the conformation or charge distribution of these aglycon derivatives. Since lipophilicity can be an important contributing factor to biological activity, we performed logP calculations for compounds **2**, **15** and **18** (Table 3.) It can be seen that compounds **2** and **18**, which possess comparable anti-influenza virus activity, have almost identical logP values. The inactive derivative **15** is more lipophilic with a logP value that is half order of magnitude higher. This suggests that for this group of glycopeptide derivatives, there is an optimum lipophilicity to obtain inhibition of influenza virus.

**Table 3.** Calculated logP values for the 4-phenylbenzyl squaramide-derivatives **2**, **15** and **18**

**ECD, NMR and Computational studies**

For the sake of simplicity, compounds ristocetin aglycon **1**, teicoplanin aglycon methyl ester **14**, and didechloro teicoplanin aglycon methyl ester **17** were chosen for the instrumental and theoretical studies (Fig 2).

**Figure 2**. Structure and numbering for ristocetin aglycon **1**, teicoplanin aglycon methyl ester **14**, and didechloro teicoplanin aglycon methyl ester **17**

Since electronic circular dichroism (ECD) spectra usually are very informative for the stereostructure, ECD spectra of the three aglycons were recorded in water. The ECD spectra of aglycoristocetin **1** and didechloro teicoplanin aglycon methyl ester **17** were nearly identical with negative Cotton effects (CE) at 244 and 288 nm accompanied by a positive CE at 202 nm with a shoulder at 212 nm for **1** (Fig 3).

**Figure 3**. ECD spectra of ristocetin aglycon **1**, teicoplanin aglycon methyl ester **14**, and didechloro teicoplanin aglycon methyl ester **17**, recorded in water

The similar ECD curves of **1** and **17** prove that they adopt a similar conformation regarding the orientation of amide and aryl chromophores. In contrast, teicoplanin aglycon methyl ester **14** having two additional chloro substituents at the aryl rings showed a markedly different ECD spectrum. This is reflected in an intense positive CE at 223 nm and a negative one at 208 nm, which were missing from the ECD spectra of **1** and **17**. The two negative high-wavelength CEs also appeared in the ECD of **14**, but their shapes, relative intensities and wavelength were different. This clearly indicates that in the presence of the two chlorine atoms, the preferred conformation or conformational ensemble of the teicoplanin aglycon **14** significantly differs from the conformation of aglycoristocetin **1**, and upon removal of the chlorine atoms, compound **17** adopts a conformation very similar to that of **1**.

**Conformational analysis at MM level**

Clustering of the low-energy 42 kJ/mol part of the GAFF (General Amber Force Field) [17,18] optimized high-temperature in vacuo molecular dynamics trajectory resulted 207, 204 and 145 clusters for **1**, **14** and **17**, respectively. ESP (Merz–Kollman) charges [19,20] were computed for the lowest-energy conformers of the three aglycons at HF/6-31G(d) level (see Fig. S1 in the SI). Basically, there were only small differences in the charge distribution of the three aglycons, indicating that the experimentally observed differences can not be mainly from the result of electronic background.

**Figure 4.** Comparison of the lowest-energy MM conformers of a) ristocetin aglycon **1** (blue) and didechloro teicoplanin aglycon methyl ester **17** (red), b) ristocetin aglycon **1** (blue) and teicoplanin aglycon methyl ester **14** (red)

Comparing the global minima obtained at GAFF level in vacuo by superimposing the lowest-energy conformers (Fig 4), structures of **1** and **17** were highly similar, while there were minor differences between **1** and **14** mostly in residues 5 and 7 (numbering is given in Fig. 2). Comparison of all low-level conformers of the three aglycons yielded similar results than the global minima, i.e. **1** and **17** are rather similar and differ from **14**, and the difference is mainly contributed to residues 5 and 7 in both cases. However, the place of conformational differnce

varies within these 2 residues in the global minima vs. in the whole considered low-energy regions. (See Figs S2 and S3 in the SI)

**Reoptimization at DFT level with solvent model**

All low-energy conformers resulted by the above mentioned clustering were reoptimized at B3LYP/6-31G level with PCM solvent model for water. In line with the MM results, the conformers of DFT global minima of **1** and **17** were very similar, while there were minor differences from **14** mostly in residues 1 and 3 (see Fig. 5). These latter results are in agreement with previous observations known from the literature, i.e. residues 5 and 7 seemed to be rather rigid in normal temperature dynamics simulations with explicit water, while 1 and 3 showed a certain level of flexibility [21]. It is interesting to note that global minima of **1** and **17** obtained after DFT reoptimization exhibit *cis* bond between residues 5 and 7 which is well known in the literature [22]. On the other hand, in the case of **14** the lowest-energy conformer with the same *cis* bond is only the $6^{th}$ lowest one after the same reoptimization. Although DFT levels can have a certain error rate and the basic set applied here is rather small because of the size of the molecules, it is very likely that the overall population of *trans* isomers in **14** is much higher than for the two other aglycons.

**Figure 5.** Comparison of the lowest-energy B3LYP/6-31G PCM/$H_2O$ conformers of a) ristocetin aglycon **1** (blue) and didechloro teicoplanin aglycon methyl ester **17** (red), b) ristocetin aglycon **1** (blue) and teicoplanin aglycon methyl ester **14** (red)

In order to support the theoretical calculations, NOESY experiments were carried out for interproton distance determinations. Because of the limited dynamic range of the NOE spectra, distances longer than 3.3 Å could not be obtained. In Tables 6-8, NMR NOE distances are compared to interproton distances from DFT (B3LYP/6-31G, PCM/H2O) reoptimized MD calculations, and the lowest energy conformer was arbitrarily chosen for comparison.The qualitative agreement is generally acceptable, however in a few cases the NMR experimental distances underestimate the distances from MD calculations.

It is worth mentioning that the NMR studies were done in DMSO while the ECD spectra were recorded in water. In DMSO ECD can be measured only down to ca. 230 nm while in water we could get good spectra down to 190 nm. Since there are main differences in the ECD spectra of **17** vs. **1** and **14** between 210 and 220 nm, DMSO can not be applied as a solvent

for ECD measurements. Furthermore, conformers in DMSO are hard to compute because of the strong complex-formation feature of this solvent [23].

**Computed ECD spectra**

ECD spectra of the DFT reoptimized global minima of **14**, **1** and **17**, and the lowest-energy *cis* isomer of **14** were computed at B3LYP/6-31G and B3LYP/6-31G(d) levels of theory with PCM solvent model for water as well as at the semiempirical ZINDO level in vacuo (since ZINDO can not handle chlorine it was changed to fluorine in **14** at this level). To check the influence of the halogen on the ECD spectra, Cl (or F) was replaced by hydrogen in **14** (**14**-H) and halogen was introduced in the corresponding positions of **17** (**17**-Cl / **17**-F). Addition or removal of halogens without reoptimizations of the original geometries did not induce a remarkable change in the computed ECD spectra, which suggested that the differences of the experimental ECD curves should derive from the different conformational ensemble of the studied derivatives (Fig 6). Thus, the difference of the ECD curves cannot be attributed exclusively to the presence of halogen atoms, which may theoretically change the direction of the electric transition moments of the interacting aryl chromophores.

**Figure 6**. ZINDO computed ECD spectra of **14-F** vs. **14-H** obtained without reoptimization of the lowest-energy conformer of **14** (left) and those of **17** and **17-F** obtained without reoptimization of the lowest-energy conformer of **17** (right)

Computed spectra of **1** and **17** were rather similar in accordance with the experimental data, while those of **14** were markedly different (see Figs S4 – S6 in the SI). Although the computed ECD spectra reproduced the major ECD transitions, they did not allow an unambiguous verification of the conformational distribution.

**Summary**

Based on this systematic structure – anti-influenza virus activity study of ristocetin and teicoplanin aglycone derivatives, we proved that the presence of a lipophilic side chain is crucial for the antiviral activity. Moreover, according to our CD measurements and *in silico* studies, the conformation (and not the electron distribution) determined mostly by the presence or absence of the chloro substituents is also a determinant factor of bioactivity. Regarding influenza virus, the mode of action of **2** is related to disruption of endocytotic uptake and intracytoplasmatic trapping of the virus [10]. Although the precise molecular basis

remains to be elucidated, we here defined the optimal conformation of the glycopeptide to achieve tight binding to its target molecule. In a next step, we hope to use these findings to design even more effective anti-influenza virus derivatives of the glycopeptide antibiotic series.

**Experimental Section**

**Materials and Methods.** Unless otherwise stated the starting materials and solvents were purchased from commercial sources (Sigma-Aldrich or Fluka) and used as received. All solvents were distilled prior to use. $CH_2Cl_2$ was distilled from $P_2O_5$ and stored over 4 Å molecular sieves. Triethylamine was distilled from KOH before use. $^{1}H$ and $^{13}C$ NMR spectra were recorded at 500.13 / 125.76 MHz frequencies, respectively, with a Bruker AVANCE II-500 spectrometer at 300 K, using DMSO-$d_6$, as solvent and TMS (tetramethylsilane) as internal standard. $^{1}H$ 90$^{o}$ pulses were typically 11 us, while the $^{13}C$ 90$^{o}$ pulse was 15 us. Signal assignments were aided by 2D HSQC, COSY, TOCSY (15 and 60 ms mixing times) and HMBC (60 ms mixing time) experiments. For interproton distance determinations 2D NOESY experiments equipped with an extra 6 ms spin-echo were run using 200 ms mixing time. NOE distance estimations were obtained by the internal reference method, using the 1.8 Å geminal proton (z2) or ortho protons in aromatic rings as reference distance. NMR spectra were processed with Bruker Topspin 3.0 software. CD spectra were recorded on a JASCO J-810 spectropolarimeter using water as solvent. Mass spectra were recorded with a Bruker Biflex-III MALDI TOF mass spectrometer. For column chromatography Merck silica gel (Kieselgel 60), 0.063-0.20 0 mm (70-230 mesh) was used. Thin layer chromatography (TLC) was performed on Kieselgel 60 $F_{254}$ (Merck), using UV light and Pauly's reagent for visualization of the spots. Evaporations were carried out under diminished pressure at 35-45 °C (bath temperature).

**Computational section**

The three aglycons were constructed utilizing the NMR refined structure of vancomycin derivative 1GAC from the PDB database. The molecular dynamics simulations (100 ns, 1200 K constant temperature, 1 fs time step) and the preliminary geometry optimizations using the suitably developed GAFF empirical force field on the equidistantly saved 200,000 trajectory snapshot geometries were carried out by means of the AMBER molecular dynamics simulation package.[24, 25] The first 42 kJ part of the optimized geometries were clustered with the MacroModel 9.7.211[26] software for heavy atoms with a 0.5 Å cut off without

reoptimization. Geometry optimizations [B3LYP/6-31G with PCM solvent model for water] and ECD calculations were performed with Gaussian 09 [27] at B3LYP/6-31G, B3LYP/6-31G(d) and ZINDO levels. ECD spectra were generated as the sum of Gaussians [28] with 2100 and 900 $cm^{-1}$ half-height width (corresponding to 12 and 5 nm at 240 nm, respectively) using dipole-velocity computed rotational strengths. The Chimera [29] and GaussView [30] software packages were used for visualization of the results.

The logP values were calculated based on the model proposed by Tetko et al. [31, 32] using the ALOGPS 2.1 web server http://www.vcclab.org/lab/alogps/ (accessed: 2015/02/04).

**Synthesis**

*General method for preparation of the squaric acid derivatives **6**, **10**, and **12**.*

To a solution of amine (0.1 mmol) in 10 mL of methanol triethylamine was added to adjust pH level between 7 and 7.5. After addition of squaric acid **5** (0.13 mmol), the solution was stirred for 20 hours at room temperature, and was evaporated in vacuum. The crude products were purified by flash column chromatography (**10**: toluene – methanol = 1 : 1; **12**: toluene – methanol – acetic acid = 5 : 5 : 0.01; the other products were used on as crude materials in the following steps) to yield the appropiate squaric acid derivatives (**10**: 52%; **12**: 71% over two steps).

**10**: MALDI-TOF MS [M+$Na^+$]: 1547.25 Da; Calcd for $C_{72}H_{62}Cl_2N_8O_{26}Na^+$: 1547.30.

**12**: MALDI-TOF MS [M+$Na^+$]: 1332.20 Da; Calcd for $C_{63}H_{49}Cl_2N_7O_{21}Na^+$: 1332.23.

*General method for preparation of the 4-phenylbenzyl derivatives **8**, **11**, **13**, **15** and **18**.*

To a solution of a squaric acid derivative (0.05 mmol) in 5 mL of methanol triethylamine was added to adjust pH level between 8 and 9. After addition of 4-phenylbenzylamine **7** (0.075 mmol), the solution was stirred for 20 hours at room temperature, and was evaporated in vacuum. The crude products were purified by flash column chromatography (**11**: toluene – methanol – acetic acid = 5 : 5 : 0.01; **13**: toluene – methanol – acetic acid = 7 : 3 : 0.01; **15**: DCM – methanol = 8 : 2; **18**: toluene – methanol = 8 : 2; in the case of **8**, column chromatography was not necessary, the precipitated product was washed with cold methanol and dry ether) to yield the appropiate 4-phenylbenzyl derivatives (**8**: 63%; **11**: 57%; **13**: 64%; **15**: 28% over two steps; **18**: 21% over two steps).

**8**: MALDI-TOF MS [M+$Na^+$]: 1684.43 Da; Calcd for $C_{83}H_{69}Cl_2N_9O_{25}Na^+$: 1684.37.

**11**: MALDI-TOF MS [M+$Na^+$]: 1698.49 Da; Calcd for $C_{84}H_{71}Cl_2N_9O_{25}Na^+$: 1698.38.

**13**: MALDI-TOF MS [M+$Na^+$]: 1483.24 Da; Calcd for $C_{75}H_{58}Cl_2N_8O_{20}Na^+$: 1483.30.

**15**: MALDI-TOF MS [M+$Na^+$]: 1497.23 Da; Calcd for $C_{67}H_{60}Cl_2N_8O_{23}Na^+$: 1497.32.

**18**: MALDI-TOF MS [M+$Na^+$]: 1429.38 Da; Calcd for $C_{76}H_{62}N_8O_{20}Na^+$: 1429.40.

*General method for preparation of the methyl esters **9**, **14**, and **17**.*

0.1 mmol of the free acid was dissolved in a mixture of 1.25 M HCl solution in methanol and methanol (1:10, 20 mL). The mixture was stirred under reflux for 1.5 hour and was evaporated in vacuum. The crude products were purified by flash column chromatography (toluene – methanol – acetic acid = 6 : 4 : 0.01) to yield the appropiate methyl ester products (**9**: 69%; **14**: 45% over two steps; **17**: 64 % over two steps).

**9**: MALDI-TOF MS [M+$Na^+$]: 1437.55 Da; Calcd for $C_{67}H_{60}Cl_2N_8O_{23}Na^+$: 1437.30.

**14**: MALDI-TOF MS [M+$Na^+$]: 1234.22 Da; Calcd for $C_{59}H_{47}Cl_2N_7O_{18}Na^+$: 1234.22.

**17**: MALDI-TOF MS [M+$Na^+$]: 1166.50 Da; Calcd for $C_{59}H_{49}N_7O_{18}Na^+$: 1166.30.

*Cleavage of the N-acetyl-D-glucosamine moiety from pseudo teicoplanin aglycon derivatives **4** and **16**.*

The solution of the *N*-acetyl-D-glucosamine derivative (0.2 mmol) in 5 mL of 90% trifluoroacetic acid was stirred for 8 hour at 80 °C. The cooled mixture was poured into 100 mL of cold ether, the product was filtered out and dried. The crude products were used for further conversions.

*Dechlorination process of **4.***

To the solution of teicoplanin pseudoaglycon **4** (0.1 mmol) in 7 mL of methanol and 3 mL of 0,04 M HCl solution 100 mg of 10 % Pd/C catalyst was added and the mixture was kept first under 1 atm pressure for 4 hours, then overnight under 5 atm with additional 200 mg of Pd/C catalyst in 4 mL of water. The reaction mixture was filtered through Cetite® and was evaporated in vacuum to yield compound **16** (72%).

**16**: MALDI-TOF MS [M+$Na^+$]: 1355.57 Da; Calcd for $C_{66}H_{60}N_8O_{23}Na^+$: 1355.37.

**NMR analysis**

**Figure 7**. Numbering atoms in teicoplanin derivatives

**Table 4**. $^1$H NMR data (chemical shifts in ppm)

**Table 5**. $^{13}C$ NMR data (chemical shifts in ppm)

**Table 6**. Measured and calculated distances of the proton pairs giving NOE in compound **1** (Interproton distances in Å). The lowest energy conformer was arbitrarily chosen for comparison.

**Table 7**. Measured and calculated distances of the proton pairs giving NOE in compound **14** (Interproton distances in Å). The lowest energy conformer was arbitrarily chosen for comparison.

**Table 8**. Measured and calculated distances of the proton pairs giving NOE in compound **17** (Interproton distances in Å). The lowest energy conformer was arbitrarily chosen for comparison.

**Acknowledgment.** This work was supported by the Hungarian Research Fund (OTKA K 109208), the University of Debrecen (Bridging Fund to P. H) and a grant from the Geconcerteerde Onderzoeksacties (GOA/10/014) from the KU Leuven. T. K. and A.M. thank the Hungarian National Research Foundation (OTKA K105871) for financial support and the National Information Infrastructure Development Institute (NIIFI 10038) for computer time. This research was also supported by the European Union and the State of Hungary, co-financed by the European Social Fund in the framework of TÁMOP 4.2.4. A/2-11-1-2012-0001 'National Excellence Program' (Szentágothai fellowship A2-SZJ-TOK-13-0081 for GB). The authors thank Wim van Dam for excellent technical assistance.

**Supporting Information Available**: Antibacterial and antiviral assays, computational data, ECD and NMR spectra.

**References and notes**

[1] Cooper, R. D.; Snyder, N. J.; Zweifel, M. J.; Staszak, M. A.; Wilkie, S. C.; Nicas, T. I.; Mullen, D. L.; Butler, T. F.; Rodriguez, M. J.; Huff, B. E.; Thompson, R. C. Reductive alkylation of glycopeptide antibiotics: Synthesis and antibacterial activity. *J. Antibiot.* **1996**, *49*, 575–581.

[2] Judice, J. K.; Pace, J. L. Semi-synthetic glycopeptide antibacterials. *Bioorg. Med. Chem. Lett.* **2003**, *13*, 4165–4168.

[3] Malabarba, A.; Ciabatti, R. Glycopeptide derivatives. *Curr. Med. Chem.* **2001**, *8* 1759–1773

[4] Sztaricskai, F.; Batta, G.; Herczegh, P.; Balázs, A.; Jekő, J.; Rőth, E.; Szabó, P. T.; Kardos, S.; Rozgonyi, F.; Boda, Z. A new series of glycopeptide antibiotics incorporating a squaric acid moiety. Synthesis, structural and antibacterial studies. *J. Antibiot.* **2006**, *59*, 564–582.

[5] Gangarosa, E. J.; Johnson, T. R.; Ramos, H. S. Ristocetin-induced thrombocytopenia: site and mechanism of action. *Arch. Intern. Med.* **1960**, *105*, 83–88.

[6] Bardsley, B.; Williams, D. H.; Baglin, T. P. Cleavage of rhamnose from ristocetin A removes its ability to induce platelet aggregation. *Blood Coagul. Fibrinolysis*, **1998**, *9*, 241–244.

[7] Pintér, G.; Bereczki, I.; Batta, G.; Ötvös, R.; Sztaricskai, F.; Rőth, E.; Ostorházi, E.; Rozgonyi, F.; Naesens, L.; Szarvas, M.; Boda, Z.; Herczegh, P., Click reaction synthesis of carbohydrate derivatives from ristocetin aglycon with antibacterial and antiviral activity. *Bioorg. Med. Chem. Lett.* **2010**, *20*, 2713–2717.

[8] J. Balzarini, C. Pannecouque, E. De Clercq, A. Y. Pavlov, S.S. Printsevskaya, O.V. Miroshnikova, M. I. Reznikova, M. N. Preobrazhenskaya, Antiretroviral activity of semisynthetic derivatives of glycopeptide antibiotics, *J. Med. Chem*. **2003**, *46*, 2755–2764.

[9] Naesens, L.; Vanderlinden, E.; Rőth, E.; Jekő, J.; Andrei, G.; Snoeck, R.; Pannecouque, C.; Illyés, E.; Batta, G.; Herczegh, P.; Sztaricskai, F.; Anti-influenza virus activity and structure–activity relationship of aglycoristocetin derivatives with cyclobutenedione carrying hydrophobic chains. *Antiviral Res.* **2009**, *82*, 89–94.

[10] Vanderlinden, E.; Vanstreels, E.; Boons, E.; ter Veer, W.; Huckriede, A, Daelemans, D.; Van Lommel, A.; Rőth, E.; Sztaricskai, F.; Herczegh, P.; Naesens, L. Intracytoplasmic trapping of influenza virus by a lipophilic derivative of aglycoristocetin. *J. Virol.* **2012**, *86*, 9416–9431.

[11] Wanner, J.; Tang, D.; McComas, C. C.; Crowley, B. M.; Jiang, W.; Moss, J.; Boger, D. L. *Bioorg. Med. Chem. Lett*. **2003**, *13*, 1169–1173.

[12] Pintér, G.; Batta, G.; Kéki, S.; Mándi, A.; Komáromi, I.; Takács-Novák, K.; Sztaricskai, F.; Rőth, E.; Ostorházi, E.; Rozgonyi, F.; Naesens, L.; Herczegh, P., Diazo transfer−click reaction route to new, lipophilic teicoplanin and ristocetin aglycon derivatives with high antibacterial and anti-influenza virus activity: an aggregation and receptor binding study. *J. Med. Chem.* **2009**, *52*, 6053–6061.

[13] Sipos, A.; Máté, G.; Rőth, E.; Borbás, A.; Batta, G.; Bereczki, I.; Kéki, S.; Jóna, I.; Ostorházi, E.; Rozgonyi, F.; Vanderlinden, E.; Naesens, L.; Herczegh, P. Synthesis of

fluorescent ristocetin aglycon derivatives with remarkable antibacterial and antiviral activities. *Eur. J. Med. Chem*. **2012**, *58*, 361–367.

[14] Sipos, A.; Török, Z.; Rőth, E.; Kiss-Szikszai, A.; Batta, G.; Bereczki, I.; Fejes, Z.; Borbás, A.; Ostorházi, E.; Rozgonyi, F.; Naesens, L.; Herczegh, P., Synthesis of isoindole and benzoisoindole derivatives of teicoplanin pseudoaglycon with remarkable antibacterial and antiviral activities. *Bioorg. Med. Chem. Lett.* **2012**, *22*, 7092–7096.

[15] Tollas, S.; Bereczki, I.; Sipos, A.; Rőth, E.; Batta, G.; Daróczi, L.; Kéki, S.; Ostorházi, E.; Rozgonyi, F.; Herczegh, P. Nano-sized clusters of a teicoplanin ψ-aglycon-fullerene conjugate. Synthesis, antibacterial activity and aggregation studies, *Eur. J. Med. Chem.* **2012**, *54*, 943–948.

[16] Tietze, L. F.; Arlt, M.; Beller, M.; Glüsenkamp, K.-H.; Jahde, E.; Rajewski, M. F. Squaric acid diethyl ester: a new coupling reagent for the formation of drug biopolymer conjugates. Synthesis of squaric acid ester amides and diamides. *Chem. Ber*. **1991**, *124*, 1215–1221.

[17] Wang, J.; Wang, W.; Kollman P. A.; Case, D. A. Automatic atom type and bond type perception in molecular mechanical calculations. *J. Mol. Graphics and Modell.* **2006**, *25*, 247–260.

[18] Wang, J.; Wolf, R. M.; Caldwell, J. W.; Kollman, P. A.; Case, D. A. Development and testing of a general AMBER force field. *J. Comput. Chem.***2004**, *25*, 1157–1174.

[19] Singh, U. C.; Kollman, P. A. An approach to computing electrostatic charges for molecules. *J. Comput. Chem.* **1984**, *5*, 129–145.

[20] Besler, B. H.; Merz Jr, K. M.; Kollman, P. A. Atomic charges derived from semiempirical methods. *J. Comput. Chem.* **1990**, *11*, 431–439.

[21] a) Jusuf, S.; Axelsen, P. H. Synchronized Conformational Fluctuations and Binding Site Desolvation during Molecular Recognition. *Biochemistry* **2004**, *43*, 15446–15452; b) Batta, G.; Sztaricskai, F.; Makarova, M. O.; Gladkikh, E. G.; Pogozheva, V. V.; Berdnikova, T. F. Backbone dynamics and amide proton exchange at the two sides of the eremomycin dimer by N-15 NMR. *Chem. Comm. 2001*, 501–502.

[22] Kövér, K. E.; Szilágyi, L.; Batta, G.; Uhrin, D.; Jiménez-Barbero, J. NMR of Glycopeptide (Vancomycin-Type) Antibiotics: Structure and Interaction with Cell Wall Analogue Peptides In: *Biomolecular Recognition by Oligosaccharides and Glycopeptides: The NMR Point of View*: Chapter 9.07 Mander LN (editor) Comprehensive Natural Products II - Chemistry and Biology, *Vol. 9*: Modern methods for the investigation of natural products. 793 p. Amsterdam: Elsevier, **2010**. pp. 197–246. (ISBN: 9780080453910)

[23] Nicu, V. P.; Baerends, E. J.; Polavarapu, P. L. Understanding Solvent Effects in Vibrational Circular Dichroism Spectra: [1,1′-Binaphthalene]-2,2′-diol in Dichloromethane, Acetonitrile, and Dimethyl Sulfoxide Solvents. *J. Phys. Chem. A* **2012**, *116*, 8366−8373.

[24] Case, D. A.; Darden, T. A.; Cheatham, T. E., III.; Simmerling, C. L.; Wang, J.; Duke, R. E.; Luo, R.; Crowley, M.; Walker, R. C.; Zhang, W.; Merz, K. M.; Wang, B.; Hayik, S.; Roitberg, A.; Seabra, G.; Kolossváry, I.; Wong, K. F.; Paesani, F.; Vanicek, J.; Wu, X.; Brozell, S. R.; Steinbrecher, T.; Gohlke, H.; Yang, L.; Tan, C.; Mongan, J.; Hornak, V.; Cui, G.; Mathews, D. H.; Seetin, M. G.; Sagui, C.; Babin, V.; Kollman, P.A. AMBER 10; University of California: San Francisco, **2008**.

[25] Jakab, Zs.; Mándi, A.; Borbás, A.; Bényei, A.; Komáromi, I.; Lázár, L.; Antus, S.; Lipták, A. Synthesis, regioselective hydrogenolysis, partial hydrogenation, and conformational study of dioxane and dioxolane-type (9′-anthracenyl)methylene acetals of sugars. *Carbohydr. Res.* **2009**, *344*, 2444–2453.

[26] MacroModel; Schrödinger LLC, 2009; http://www.schrodinger.com/productpage/14/11/.

[27] Frisch, M. J.; Trucks, G. W.; Schlegel, H. B.; Scuseria, G. E.; Robb, M. A.; Cheeseman, J. R.; Scalmani, G.; Barone, V.; Mennucci, B.; Petersson, G. A.; Nakatsuji, H.; Caricato, M.; Li, X.; Hratchian, H. P.; Izmaylov, A. F.; Bloino, J.; Zheng, G.; Sonnenberg, J. L.; Hada, M.; Ehara, M.; Toyota, K.; Fukuda, R.; Hasegawa, J.; Ishida, M.; Nakajima, T.; Honda, Y.; Kitao, O.; Nakai, H.; Vreven, T.; Montgomery, J. A.; Peralta, J. E. Jr.; Ogliaro, F.; Bearpark, M.; Heyd, J. J.; BRőthers, E.; Kudin, K. N.; Staroverov, V. N.; Kobayashi, R.; Normand, J.; Raghavachari, K.; Rendell, A.; Burant, J. C.; Iyengar, S. S.; Tomasi, J.; Cossi, M.; Rega, N.; Millam, J. M.; Klene, M.; Knox, J. E.; Cross, J. B.; Bakken, V.; Adamo, C.; Jaramillo, J.; Gomperts, R.; Stratmann, R. E.; Yazyev, O.; Austin, A. J.; Cammi, R.; Pomelli, C.; Ochterski, J. W.; Martin, R. L.; Morokuma, K.; Zakrzewski, V. G.; Voth, G. A.; Salvador, P.; Dannenberg, J. J.; Dapprich, S.; Daniels, A. D.; Farkas, O.; Foresman, J. B.; Ortiz, J. V.; Cioslowski, J.; Fox, D. J. Gaussian 09, revision B.01; Gaussian, Inc.: Wallingford CT, 2010.

[28] Stephens, P. J.; Harada, N. ECD cotton effect approximated by the Gaussian curve and other methods. *Chirality* **2010**, *22*, 229–233.

[29] Pettersen, E. F.; Goddard, T. D.; Huang, C. C.; Couch, G. S.; Greenblatt, D. M.; Meng, E. C.; Ferrin, T. E. *J. Comput. Chem.* **2004**, *25*, 1605–1612.

[30] Dennington, R.; Keith, T.; Millam, J. GaussView, Version 5, Semichem Inc., Shawnee Mission KS, **2009**.

[31] Tetko, I. V.; Tanchuk, V. Y. Application of associative neural networks for prediction of lipophilicity in ALOGPS 2.1 program. *J. Chem. Inf. Comput. Sci.*, **2002**, *42*, 1136-45.

[32] Tetko, I. V.; Tanchuk, V. Y.; Villa, A. E. Prediction of n-octanol/water partition coefficients from PHYSPROP database using artificial neural networks and E-state indices, *J. Chem. Inf. Comput. Sci.*, **2001**, *41*, 1407-21.

Figures, Schemes and Tables of the manuscript:

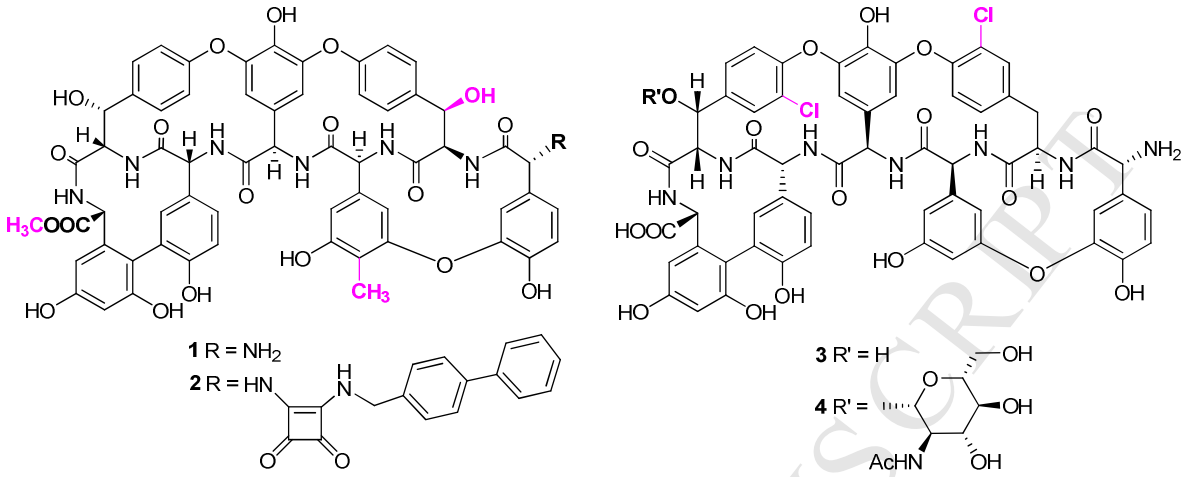


**Figure 1**. Structures of ristocetin aglycon **1**; its *N*-terminally modified derivative **2** which has potent and broad-activity against influenza virus; teicoplanin aglycon **3**; and teicoplanin pseudoaglycon **4**. The main differences between the glycopeptide cores are highlighted in magenta.

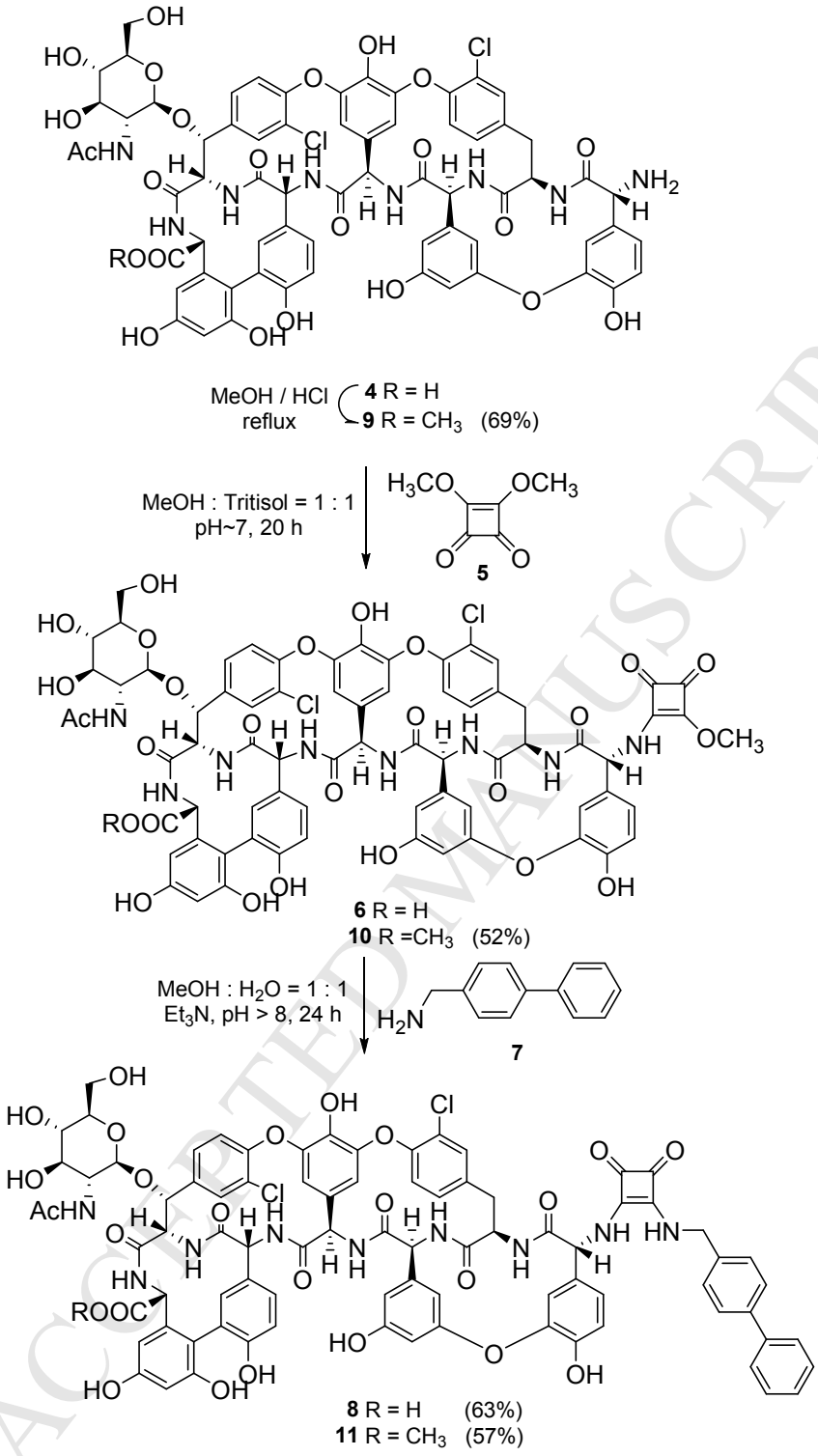


**Scheme 1**. Synthesis of **8** and **11** as teicoplanin-pseudoaglycon-counterparts of compound **2**

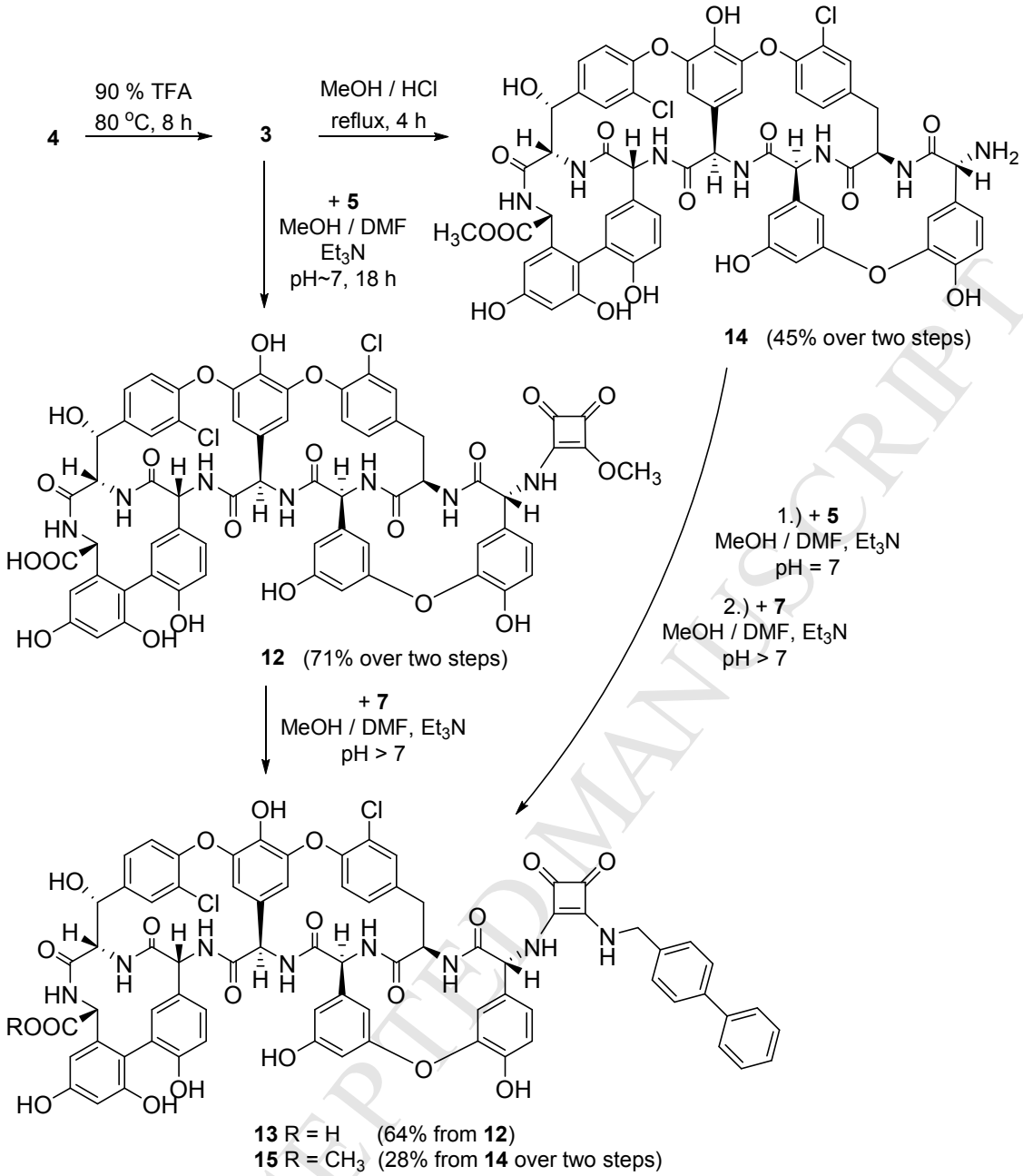


**Scheme 2**. Transformation of teicoplanin pseudoaglycon **4** into the *N*-terminally modified teicoplanin aglycon **13** and its methyl ester **15**

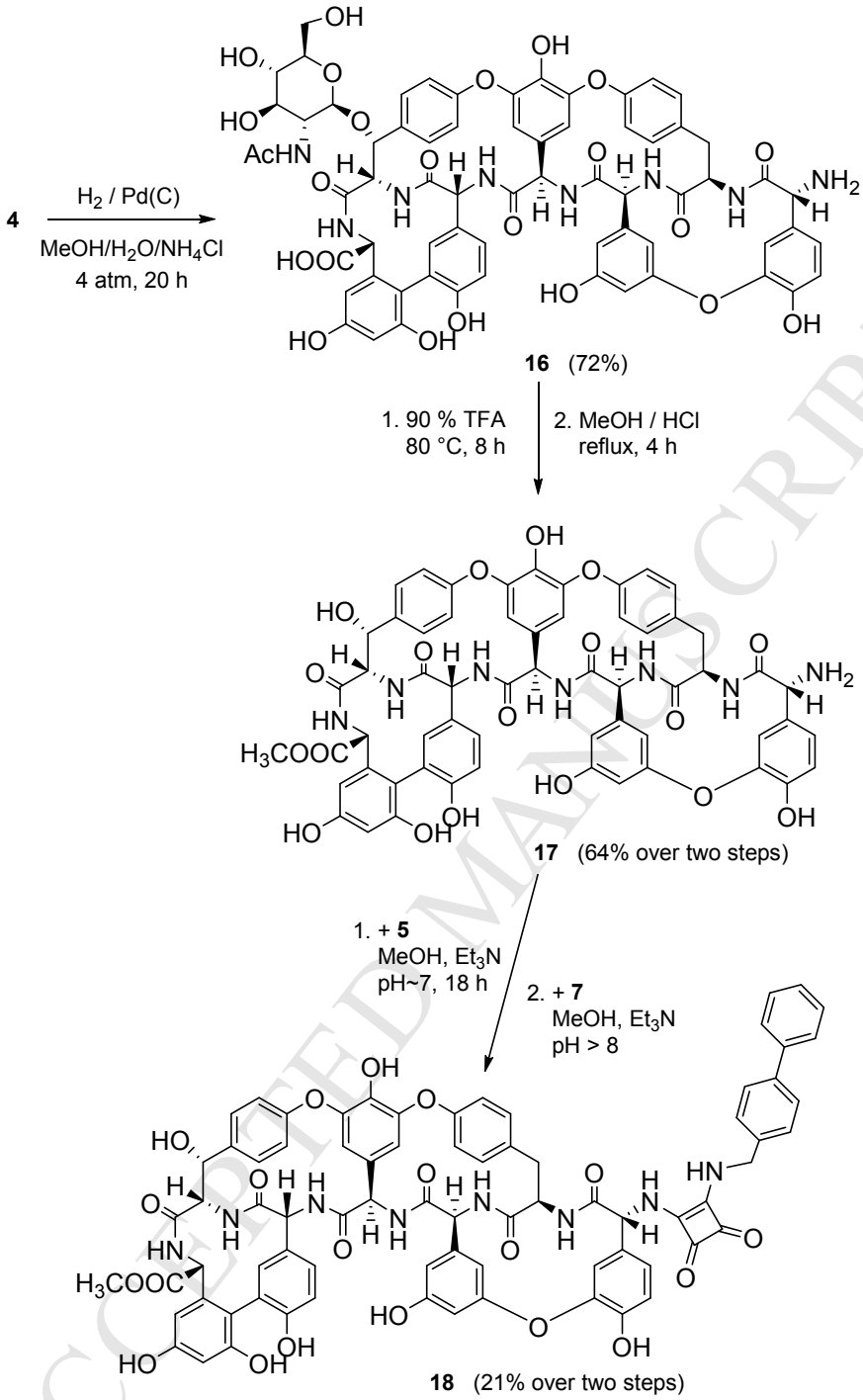


**Scheme 3**. Transformation of teicoplanin pseudoaglycon **4** into the *N*-terminally modified didechlorinated teicoplanin aglycon methyl ester **18** via didechlorinated teicoplanin aglycon methyl ester **17**

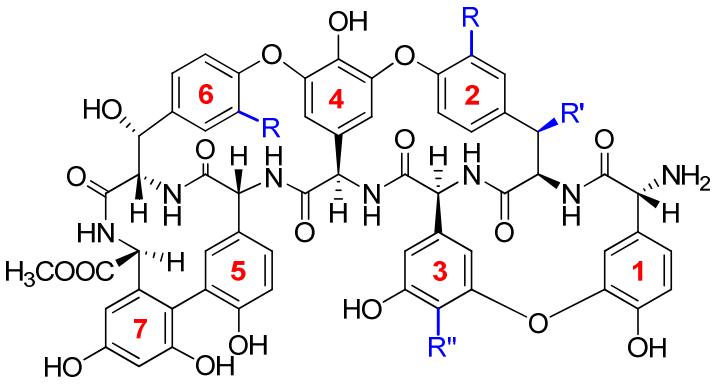


**1** R = H, R' = OH, R'' = $CH_3$
**14** R = Cl, R' = R'' = H
**17** R = R' = R'' = H

**Figure 2**. Structure and numbering for ristocetin aglycon **1**, teicoplanin aglycon methyl ester **14**, and didechloro teicoplanin aglycon methyl ester **17**

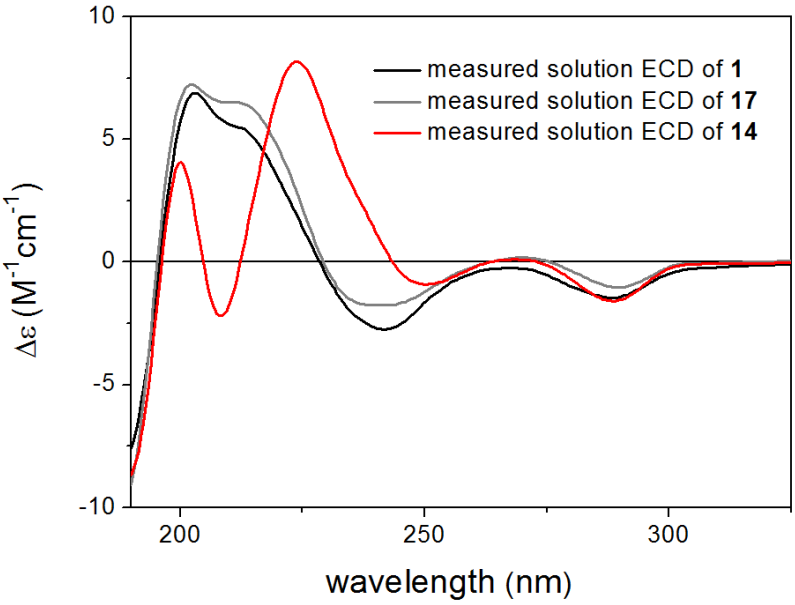


**Figure 3**. ECD spectra of ristocetin aglycon **1**, teicoplanin aglycon methyl ester **14**, and didechloro teicoplanin aglycon methyl ester **17**, recorded in water

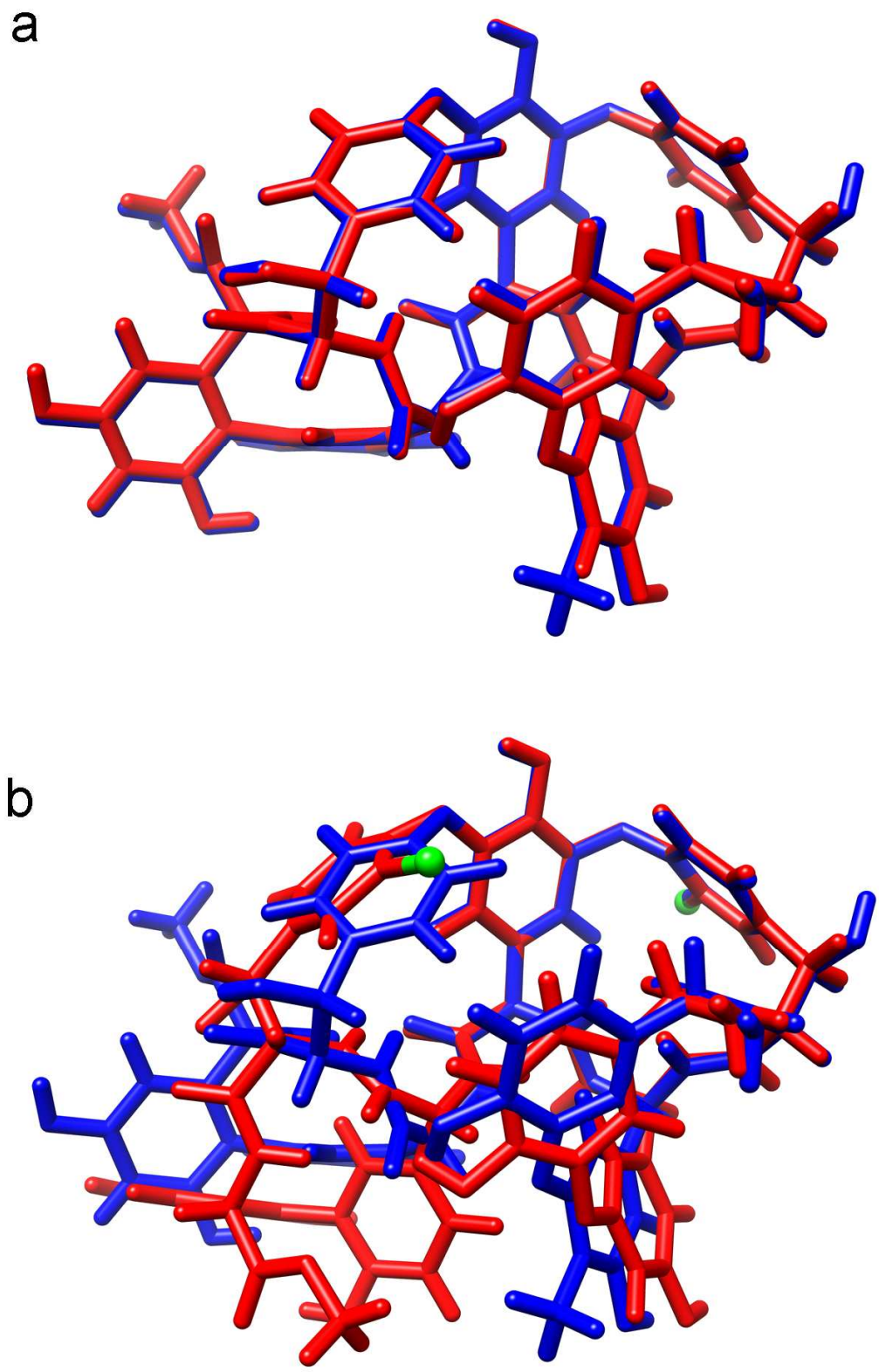


**Figure 4.** Comparison of the lowest-energy MM conformers of a) ristocetin aglycon **1** (blue) and didechloro teicoplanin aglycon methyl ester **17** (red), b) ristocetin aglycon **1** (blue) and teicoplanin aglycon methyl ester **14** (red)

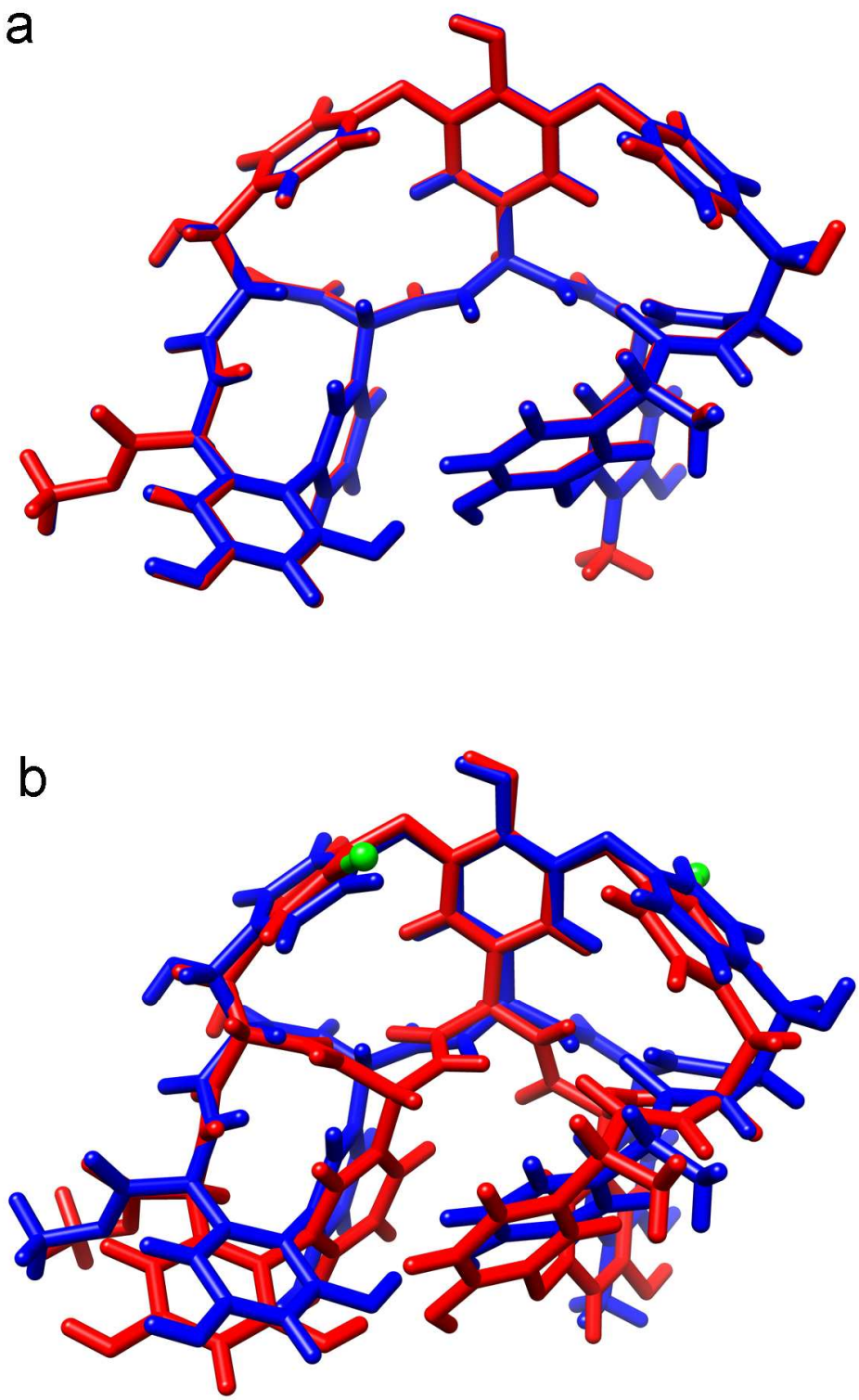


**Figure 5.** Comparison of the lowest-energy B3LYP/6-31G PCM/$H_2O$ conformers of a) ristocetin aglycon **1** (blue) and didechloro teicoplanin aglycon methyl ester **17** (red), b) ristocetin aglycon **1** (blue) and teicoplanin aglycon methyl ester **14** (red)

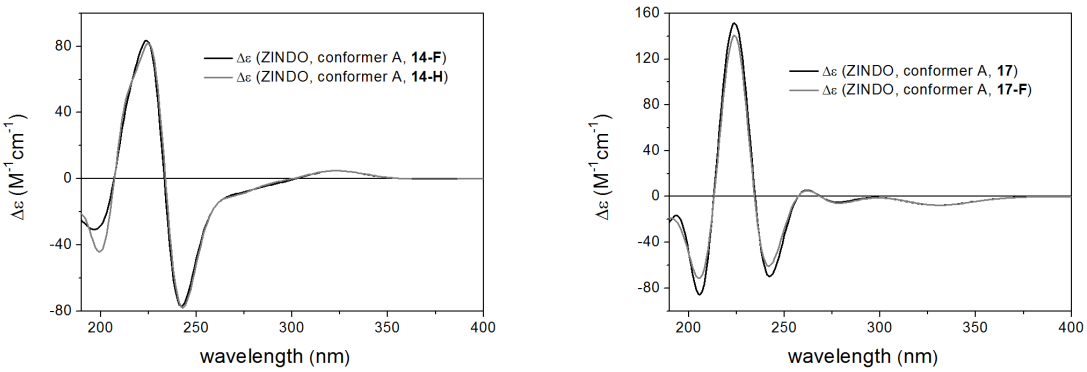


**Figure 6**. ZINDO computed ECD spectra of **14-F** vs. **14-H** obtained without reoptimization of the lowest-energy conformer of **14** (left) and those of **17** and **17-F** obtained without reoptimization of the lowest-energy conformer of **17** (right)

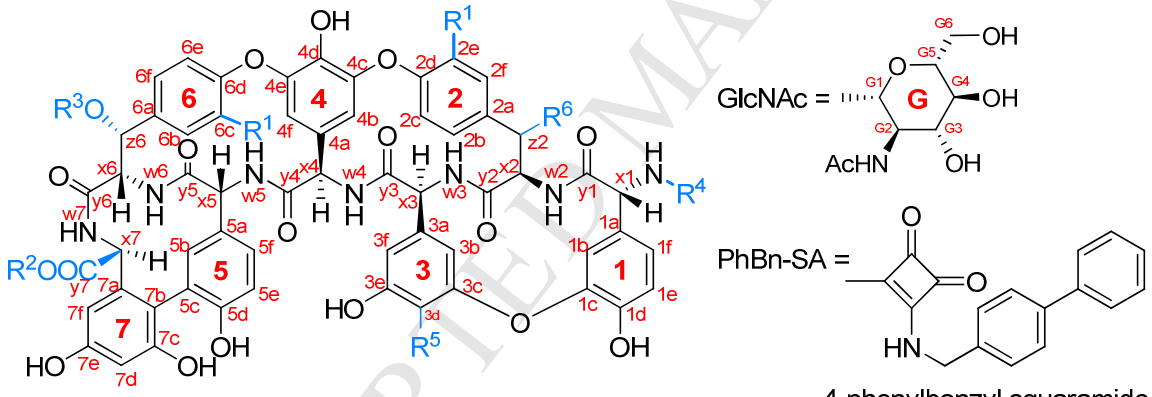


**1:** $R^1 = R^3 = R^4 = H$, $R^2 = R^5 = CH_3$, $R^6 = OH$
**3**: $R^1 = Cl$, $R^2 = R^3 = R^4 = R^5 = R^6 = H$
**4**: $R^1 = Cl$, $R^2 = R^4 = R^5 = R^6 = H$, $R^3 = GlcNAc$
**8**: $R^1 = Cl$, $R^2 = R^5 = R^6 = H$, $R^3 = GlcNAc$, $R^4 = PhBn\text{-}SA$
**13**: $R^1 = Cl$, $R^2 = R^3 = R^5 = R^6 = H$, $R^4 = PhBn\text{-}SA$
**14**: $R^1 = Cl$, $R^2 = CH_3$, $R^3 = R^4 = R^5 = R^6 = H$
**17**: $R^1 = R^3 = R^4 = R^5 = R^6 = H$, $R^2 = CH_3$
**18**: $R^1 = R^3 = R^5 = R^6 = H$, $R^2 = CH_3$, $R^4 = PhBn\text{-}SA$

**Figure 7**. Numbering atoms in teicoplanin derivatives

**Table 1.** Antibacterial activity of the synthesized compounds

| Strains | MIC (µg/mL) | | | | | | | | | | |
|---|---|---|---|---|---|---|---|---|---|---|---|
| | **Teicoplanin** | **Ristocetin** | **2** | **8** | **9** | **10** | **11** | **12** | **13** | **15** | **18** |
| *Bacillus subtilis* ATCC 6633 | 0.5 | 16 | 2 | 4 | 0.5 | 8 | 8 | 16 | 8 | 256 | 16 |
| *Staphylococcus aureus* MSSA ATCC 29213 | 0.5 | 128 | 1 | 1 | 0.5 | 2 | 2 | 1 | 2 | 128 | 8 |
| *Staphylococcus aureus* MRSA ATCC 33591 | 0.5 | 32 | 8 | 4 | 1 | 8 | 0.5 | 2 | 2 | 256 | 32 |
| *Staphylococcus epidermidis* mecA | 16 | 128 | 2 | 1 | 0.5 | 8 | 0.5 | 2 | 2 | 32 | 8 |
| *Staphylococcus epidermidis* biofilm ATCC 35984 | 4 | 2 | 2 | 1 | 0.5 | 4 | 0.5 | 2 | 0.5 | 256 | 32 |
| *Enterococcus faecalis* ATCC 29212 | 1 | 4 | 1 | 4 | 2 | 2 | 0.5 | 4 | 1 | 64 | 4 |
| *Enterococcus faecalis* 15376 vanA+ | 256 | 16 | n.d. | 256 | 0.5 | 0.5 | 0.5 | 2 | 1 | 128 | 16 |
| *Enterococcus faecalis* ATCC 51299 vanB+ | 0.5 | 256 | 8 | 8 | 1 | 4 | 0.5 | 8 | 8 | 256 | 4 |

MIC: Minimum Inhibitory Concentration; ATCC: American Type Culture Collection; vanA+: vanA gene positive; MSSA: Methicillin Sensitive *Staphylococcus;* mecA: mecA gene expression in *Staphylococcus;* vanB+: vanB gene positive; MRSA: Methicillin Resistant *Staphylococcus aureus; n.d. not determined*.

**Table 2.** Activity in influenza virus-infected MDCK[a] cells

| Compound | Cytotoxicity[b] | | Antiviral $EC_{50}$[c] | | | | | |
|---|---|---|---|---|---|---|---|---|
| | | | A/H1N1 A/PR/8/34 | | A/H3N2 A/HK/7/87 | | Influenza B B/HK/5/72 | |
| | MCC | $CC_{50}$ | CPE | MTS | CPE | MTS | CPE | MTS |
| | (μM) | | | | | | | |
| Ristocetin aglycon (**1**) | 81 | 44 | n.d. | n.d. | 4.6 | 2.5 | 5.1 | 5.4 |
| Teicoplanin ψ-aglycon (**4**) | ≥ 100 | > 100 | 23 | 43 | 17 | 34 | > 100 | > 100 |
| **2** | 20 | 39 | 0.15 | 0.21 | 0.15 | ≤ 0.42 | 0.84 | 1.0 |
| **3** | 100 | > 100 | > 100 | > 100 | > 100 | > 100 | > 100 | > 100 |
| **8** | 0.8 | 6.5 | > 100 | > 100 | > 100 | > 100 | > 100 | > 100 |
| **9** | 100 | > 100 | > 100 | > 100 | > 100 | > 100 | > 100 | > 100 |
| **10** | 100 | > 100 | > 100 | > 100 | > 100 | > 100 | > 100 | > 100 |
| **11** | 20 | 58 | > 100 | > 100 | > 100 | > 100 | > 100 | > 100 |
| **12** | 100 | 49 | > 100 | > 100 | > 100 | > 100 | > 100 | > 100 |
| **13** | 20 | 11 | > 100 | > 100 | > 100 | > 100 | > 100 | > 100 |
| **15** | 4 | 7.6 | > 100 | > 100 | > 100 | > 100 | > 100 | > 100 |
| **18** | 16 | 20 | 0.67 | 0.58 | 0.52 | 0.70 | >100 | >100 |
| Oseltamivir carboxylate | > 100 | > 100 | 2.0 | 2.9 | 4.0 | 2.3 | 20 | 15 |
| Ribavirin | > 100 | > 100 | 9.0 | 8.9 | 12 | 12 | 7.0 | 3.4 |
| Amantadine | > 500 | > 500 | 224 | 453 | 2.0 | 1.8 | > 500 | > 500 |
| Rimantadine | > 500 | > 500 | 4.0 | 15 | 4.0 | 1.1 | > 500 | > 500 |

[a]MDCK, Madin-Darby canine kidney cells. Data shown represent the means of 2 to 5 independent tests.
[b]Cytotoxicity was expressed as the minimum cytotoxic concentration (MCC; compound concentration producing minimal changes in cell morphology, as estimated by microscopy) or the 50% cytotoxic concentration ($CC_{50}$; estimated by the MTS cell viability assay).
[c]Antiviral activity was expressed as the $EC_{50}$ defined as the compound concentration producing 50% inhibition of virus replication, as estimated by microscopic scoring of the cytopathic effect (CPE) or by measuring cell viability in the formazan-based MTS assay.
n.d.: not determined

**Table 3.** Calculated logP values for the 4-phenylbenzyl squaramide-derivatives **2**, **15** and **18**

| Compound | **2** | **15** | **18** |
|---|---|---|---|
| logP | 4.38 | 5.02 | 4.49 |

**Table 4**. $^{1}$H NMR data (chemical shifts in ppm)

| | **1*** | **3** | **4** | **8** | **13** | **14** | **17** | **18** |
|---|---|---|---|---|---|---|---|---|
| 5b | 7.12 | 7.123 | 7.059 | 7.476[a] | | 7.095 | 7.12 | |
| 2b | 7.837 | 7.22 | 7.212 | 7.166 | | 7.179 | 7.062 | |
| 2f | | 7.646 | 7.652 | | | 7.629 | 7.716 | |
| 6c | | | | | | | 6.725 | |
| 6f | 7.539 | 7.466 | 7.256 | 7.246 | 7.42 | 7.456 | 7.482 | 7.46 |
| 6b | 7.474 | 7.8 | 7.873 | 7.856 | 7.81 | 7.79 | 7.557 | 7.79 |
| 2c | | | | | | | 7.122 | |
| 5f | | 6.72 | 6.636 | 6.654 | 6.64 | 6.67 | 6.684 | 6.64 |
| 1f | | 7.125 | 7.194 | | 7.09 | 7.038 | 7.113 | |
| 2e | | 7.224 | 7.169 | 7.15[a] | 7.18 | 7.134 | 7.009 | |
| 6e | | 7.234 | 7.26 | 7.138 | 7.20 | 7.216 | 7.076 | |
| 1e | | 6.936 | 6.986 | 6.93 | 6.93 | 6.905 | 7.023 | 6.93 |
| 1b | | 6.682 | 6.736 | 6.752 | 6.74 | 6.698 | 6.816 | 6.74 |
| 5e | | 6.67 | 6.625 | 6.656 | 6.63 | 6.681 | 6.685 | 6.56 |
| 3b | 6.414 | 6.359 | 6.342 | 6.319 | 6.32 | 6.313 | 6.313 | 6.30 |
| 4b | 5.647 | 5.568 | 5.528 | 5.56 | 5.52 | 5.516 | 5.593 | 5.59 |
| 7f | 6.075 | 6.292 | 6.38 | 6.308 | | 6.05 | 6.075 | 6.03 |
| 3d | | 6.34 | 6.3 | 6.33 | 6.33 | 6.32 | 6.358 | 6.32 |
| 4f | 5.294 | 5.147 | 5.081 | 5.11 | 5.13 | 5.128 | 5.323 | 5.31 |
| 3f | 6.452 | 6.4 | 6.378 | 6.455 | 6.44 | 6.46 | 6.48 | 6.34 |
| 7d | 6.419 | 6.4 | 6.377 | 6.308 | 6.28 | 6.434 | 6.446 | 6.29 |
| Z6 | 5.126 | 5.117 | 5.295 | 5.376 | 5.16 | 5.09 | 5.115 | 5.11 |
| X6 | 4.155 | 4.14 | 4.151 | 4.173 | | 4.136 | 4.164 | |
| X3 | 5.249 | 5.358 | 5.353 | 5.343 | | 5.325 | 5.297 | 5.31 |
| X1 | 4.63 | 4.587 | 4.998 | 6.03[a] | | 4.721 | 4.787 | |
| X7 | 4.505 | 4.459 | 4.424 | 4.292 | | 4.508 | 4.505 | 3.78 |
| X4 | 5.627 | 5.631 | 5.65 | 5.618 | | 5.627 | 5.575 | 5.56 |
| X2 | 5.115 | 5.02 | 4.932 | 5.005 | | 4.996 | 4.906 | 4.97 |
| X5 | 4.397 | 4.384 | 4.286 | 4.365 | | 4.354 | 4.417 | 4.44 |
| Z2 | 5.154 | 2.869/3.321[a] | 3.338/2.815[a] | 3.25/2.86[a] | | 2.82/3.26[a] | 2.86/3.26[a] | 3.23/2.86[a] |
| Me | 3.689 | | | | | 3.689 | 3.687 | |
| | | | | | | | | |
| G-1 | | | 4.339 | 4.369 | | | | |
| G-2 | | | 3.362 | 3.528 | | | | |
| G-3 | | | 3.434 | 3.384 | | | | |
| G-4 | | | 3.078 | 3.226 | | | | |
| G-5 | | | 3.064 | 3.082 | | | | |

| | | | | | | |
|---|---|---|---|---|---|---|
| G-6 | | 3.49/3.69[a] | 3.617 | | | |
| $CH_3$ (NHAc) | | 1.889 | 1.765 | | | |
| N-$CH_2$ sidechain | | | | | | 4.77 |
| PhBn | | | 7.466 | 7.46 | | 7.46 |
| PhBn | | | 7.427 | 7.42 | | 7.43 |
| PhBn | | | 7.371 | 7.36 | | 7.36 |
| PhBn | | | 7.677 | 7.65 | | 7.66 |

*More detailed assignement of the ristocetin aglycon **1** in deuterated methanol has been published earlier [4]; a: ambiguous assignment

**Table 5**. $^{13}$C NMR data (chemical shifts in ppm)

| | **1*** | **3** | **4** | **8** | **13** | **14** | **17** | **18** |
|---|---|---|---|---|---|---|---|---|
| y1 | | 173.21 | 174.18 | 174.17 | | 172.19 | 173.21 | |
| y7 | | 172.25 | 171.32 | 171.15 | | 170.48 | 172.2 | |
| y4 | | 170.05 | 171.14 | 170.9 | | 169.86 | 170.5 | |
| y2 | | 169.06 | 169.93 | 170.37 | | 169.8 | 169.86 | |
| y5 | | 169.06 | 169.89 | 169.98 | | 168.87 | 169.82 | |
| y3 | | 168.01 | 169.07 | 169.04 | | 168.56 | 168.77 | |
| y6 | | 167.35 | 167.15 | 168.86 | | 166.71 | 168.72 | |
| 3c | | 158.44 | 159.38 | 159.42 | | 159.12 | 159.07 | |
| 7e | | 157.3 | 158.73 | 158.52 | | 158.15 | 157.93 | |
| 3e | | 157.1 | 158 | 157.81 | | 158 | 157.78 | |
| 7c | | 156.35 | 157.19 | 1569 | | 157.41 | 157.17 | |
| 5d | | 155.4 | 156.39 | 156.4 | | 156.05 | 155.91 | |
| 2d | | 150.68 | 151.74 | 151.76 | | 151.13 | 155.13 | |
| 6d | | 148.63 | 150.21 | 150.07 | | 149.3 | 155.03 | |
| 4c | | 147.61 | 149.35 | 148.98 | | 148.2 | 150.04 | |
| 4e | | 147.5 | 148.74 | 148.71 | | 147.98 | 149.75 | |
| 1d | | 146.83 | 148.44 | 148.43 | | 147.81 | 147.84 | |
| 6a | | 142.04 | 143.15 | 143.35 | | 142.52 | 142.13 | |
| 1c | | 141.47 | 141.66 | 141.71 | | 141.96 | 141.31 | |
| 3a | | 140.7 | 139.18 | 139.43 | | 141.54 | 139.9 | |
| 7a | | 136.14 | 137.76 | 138.75 | | 135.96 | 135.82 | |
| 5b | 136.12 | 135.53 | 136.58 | 136.75[a] | | 136.3 | 136.35 | |
| 2a | | 135.42 | 136.3 | 136.46 | | 135.77 | 135.29 | |
| 4d | | 134.19 | 135.18 | 135.2 | | 134.76 | 133.88 | |

| | | | | | | | | |
|---|---|---|---|---|---|---|---|---|
| 1a | | 131.48 | 128.19 | 128.23 | | 128.36 | 128.17 | |
| 2b | 128.63 | 130.9 | 131.85 | 131.92 | | 131.21 | 131.32 | |
| 2f | | 129.87 | 131.18 | 131.24 | | 131.13 | 131.9 | |
| 4a | | 127.61 | 128.82 | 128.76 | | 127.78 | 126.48 | |
| 6c | | 127.51 | 127.54 | 126.36 | | 127.78 | 121.86 | |
| 6f | 127.1 | 127.22 | 129 | 128.36 | 127.61 | 127.78 | 128.61 | 127.03 |
| 6b | 128.67 | 127.16 | 129.51 | 129.43 | 127.81 | 127.81 | 127.14 | 127.30 |
| 2c | | 126.11 | 126.76 | | | 126.63 | 124.11 | |
| 5a | | 125.83 | 126.46 | | | 126.32 | | |
| 5f | | 125.66 | 126.57 | 126.04 | 125.49 | 126.26 | 126.21 | 125.79 |
| 1f | | 124.89 | 125.73 | 125.66 | 125.83 | 125.27 | 125.09 | |
| 2e | | 124.55 | 127.02 | 124.14[a] | 125.08 | 125.13 | 123.2 | |
| 6e | | 123.08 | 124.22 | 123.3 | 123.44 | 123.72 | 121.14 | |
| 5c | | 121.13 | 122.44 | 122.71 | | 121.6 | 121.39 | |
| 1e | | 118.25 | 119.34 | 119.69 | 118.99 | 118.54 | 118.45 | 119.10 |
| 7b | | 117.69 | 118.63 | 118.66 | | 118.15 | 118.18 | |
| 1b | | 117.45 | 119.91 | 119.07 | 119.06 | 118.5 | 118.7 | 118.68 |
| 5e | | 116.52 | 117.52 | 117.33 | 116.74 | 117.13 | 117.04 | 117.45 |
| 3b | 109.86 | 110.01 | 110.86 | 110.95 | 110.31 | 110.39 | 110.21 | 110.21 |
| 4b | 107.14 | 107.18 | 108.6 | 108.52 | 10764 | 107.66 | 107.6 | 107.34 |
| 7f | 105.77 | 105.94 | 105.84 | 105.91 | | 105.68 | 105.83 | 105.15 |
| 3d | | 104.87 | 107.1 | 107.84 | 105.18 | 105.28 | 105.43 | 105.01 |
| 4f | 106.05 | 104.3 | 105.43 | 105.91 | 104.77 | 104.84 | 106.37 | 106.24 |
| 3f | 103.9 | 102.66 | 104.35 | 104.35 | 103.47 | 103.78 | 103.99 | 103.51 |
| 7d | 103.07 | 102.66 | 103.16 | 102.78 | 102.11 | 103.33 | 103.22 | 102.96 |
| Z6 | 72.3 | 71.4 | 76.78 | 76.31 | 71.68 | 71.96 | 72.35 | 72.20 |
| X6 | 62.48 | 61.63 | 61.83 | 61.53 | 62.25 | 62.2 | 62.46 | |
| X3 | 58.43 | 57.94 | 58.98 | 59.08 | 58.76 | 58.74 | 58.68 | 58.66 |
| X1 | 58.51 | 57.92 | 56.73 | 59.46[a] | | 57.87 | 57.72 | |
| X7 | 56.98 | 56.63 | 58.16 | 59.91 | 59.72 | 57 | 56.95 | 59.07 |
| X4 | 55.03 | 54.84 | 55.59 | 55.23 | 55.14 | 55.09 | 55.07 | 54.97 |
| X2 | 60.58 | 54.27 | 55.98 | 55.54 | 55.35 | 54.93 | 55.47 | 55.38 |
| X5 | 54.04 | 53.53 | 54.64 | 54.22 | 53.98 | 54.08 | 54.02 | 53.74 |
| Z2 | 71.94 | 36.69 | 37.25 | 36.95 | 37.02 | 37.51 | 37.62 | 37.33 |
| Me | | | | | | 52.26 | 52.28 | |
| | | | | | | | | |
| G-1 | | | 99.95 | 99.48 | | | | |
| G-2 | | | 56.98 | 56.26 | | | | |
| G-3 | | | 73.98 | 74.14 | | | | |
| G-4 | | | 71.62 | 71.35 | | | | |

| | | | | |
|---|---|---|---|---|
| G-5 | 77.71 | 77.73 | | |
| G-6 | 62.09 | 61.73 | | |
| 2NH-CO, G | 170.53 | | | |
| $CH_3$ (NHAc) | 24.03 | 24.12 | | |
| | | | | |
| C=O (SA) | | 183.75 | 183.36 | |
| C=O (SA) | | 183.34 | 182.97 | |
| SA | | 167.19 | | |
| SA | | 166.69 | | |
| N-$CH_2$ sidechain | | | 46.87 | 46.90 |
| PhBn | | 140.32 | | |
| PhBn | | 129.8 | 129.32 | 129.21 |
| PhBn | | 129.06 | 128.56 | 128.53 |
| PhBn | | 127.91 | 127.81 | 127.85 |
| PhBn | | 127.53 | 127.20 | 127.16 |

*More detailed assignement of the ristocetin aglycon **1** in deuterated methanol has been published earlier [4]; a: ambiguous assignment

**Table 6**. Measured and calculated distances of the proton pairs giving NOE in compound **1** (Interproton distances in Å). The lowest energy conformer was arbitrarily chosen for comparison.

| NOE pairs | Integrations of NOE cross peaks | Measured distance (NOE) | Calculated distance (B3LYP) |
|---|---|---|---|
| 1b-3b | 1.21E+008 | 2.6 | 2.5 |
| 1f-1e | 1.70E+008 | 2.5 | 2.5 |
| 2b-2c | 5.68E+007 | 3.0 | 2.5 |
| 3b-x3 | 1.05E+008 | 2.7 | 3.8 |
| 4f-x5 | 3.62E+007 | 3.2 | 3.4 |
| 5b-x5 | 1.35E+008 | 2.6 | 2.3 |
| 5b-x6 | 1.04E+008 | 2.7 | 2.7 |
| | | | |
| 6b-w6 | 2.98E+007 | 3.3 | 2.8 |
| 6f-x6 | 3.62E+007 | 3.2 | 2.6 |
| 6f-z6 | 8.58E+007 | 2.8 | 2.5 |
| | | | |
| w5-x4 | 9.44E+007 | 2.8 | 2.3 |

| | | | |
|---|---|---|---|
| w7-5b | 8.90E+007 | 2.8 | 2.2 |
| w7-x5 | 3.07E+007 | 3.3 | 3.6 |
| w7-x6 | 6.90E+007 | 2.9 | 2.3 |
| w7-z6 | 4.09E+007 | 3.2 | 3.5 |
| x5-x6 | 1.32E+008 | 2.6 | 2.1 |
| z6-x6 | 6.72E+007 | 2.9 | 2.5 |

**Table 7**. Measured and calculated distances of the proton pairs giving NOE in compound **14** (Interproton distances in Å). The lowest energy conformer was arbitrarily chosen for comparison.

| NOE pairs | Integrations of NOE cross peaks | Measured distance (NOE) | Calculated distance (B3LYP) |
|---|---|---|---|
| *1b-3b* | 2.25E+07 | 2.0 | 2.5 |
| 1b-x1 | 3.14E+06 | 2.7 | 3.7 |
| 1f-1e | 2.37E+07 | 2.0 | 2.5 |
| 1f-x1 | 7.94E+06 | 2.3 | 2.4 |
| 2b-z2a | 6.59E+06 | 2.4 | 3.6 |
| 2b-z2b | 2.19E+07 | 2.0 | 2.4 |
| 2f-2e | 1.69E+07 | 2.0 | 2.5 |
| 2f-x1 | 1.95E+06 | 3.0 | 3.9 |
| 2f-z2 | 7.84E+06 | 2.3 | 2.6 |
| *3f-x3* | 2.10E+07 | 2.0 | 4.6 |
| 4b-4f | 3.03E+06 | 2.8 | 4.3 |
| 4b-x4 | 3.77E+06 | 2.7 | 3.3 |
| *4f-x5* | 1.09E+07 | 2.2 | *4* |
| 5b-x5 | 3.51E+07 | 1.8 | 2.6 |
| *5b-x6* | 2.68E+07 | 2.0 | *3.8* |
| *5b-z6* | 3.39E+06 | 2.7 | 6.1 |
| 6b-5b | 3.44E+06 | 2.7 | 5.4 |
| *6b-x5* | 6.57E+06 | 2.4 | *4.9* |
| 6b-x6 | 1.33E+07 | 2.2 | 2.2 |
| 6b-z6 | 3.14E+07 | 1.9 | 3.1 |
| 6f-6e | 2.10E+07 | 2.0 | 2.5 |
| 6f-w6 | 8.51E+06 | 2.3 | 3.9 |
| 7f-Me | 5.81E+06 | 2.5 | 3.5 |
| 7f-w7 | 2.00E+06 | 3.0 | 3,5 |
| w5-4f | 4.57E+06 | 2.6 | 4 |

| | | | |
|---|---|---|---|
| w5-5f | 4.16E+06 | 2.6 | 3.2 |
| w5-x4 | 2.20E+07 | 2.0 | 3.5 |
| w5-x5 | 4.33E+06 | 2.6 | 2.2 |
| w7-b5 | 2.07E+07 | 2.0 | 2.6 |
| w7-b6 | 2.92E+06 | 2.8 | 4.5 |
| w7-x5 | 5.85E+06 | 2.5 | 4.5 |
| w7-x6 | 1.86E+07 | 2.0 | 2.4 |
| w7-x7 | 5.75E+06 | 2.5 | 2.9 |
| w7-z6 | 9.46E+06 | 2.3 | 4.2 |
| x2-z2 | 1.03E+07 | 2.2 | 2.5 |
| x2-z2 | 1.28E+07 | 2.2 | 2.3 |
| *x5-x6* | 4.00E+07 | 1.8 | 4.5 |
| z2a-z2b | 3.82E+07 | 1.8 | 1.8 |
| z6-x5 | 4.42E+06 | 2.6 | 6.6 |
| z6-x6 | 1.75E+07 | 2.0 | 2.4 |

**Table 8**. Measured and calculated distances of the proton pairs giving NOE in compound **17** (Interproton distances in Å). The lowest energy conformer was arbitrarily chosen for comparison.

| NOE pairs | Integrations of NOE cross peaks | Measured distance (NOE) | Calculated distance (B3LYP) |
|---|---|---|---|
| 1b-3b | 4.25E+007 | 1.8 | 2.5 |
| 1b- x1 | 3.94E+006 | 2.7 | 3.8 |
| 1f- x1 | 7.48E+006 | 2.4 | 2.4 |
| 2b- z2a | 4.20E+006 | 2.7 | 3.7 |
| 2b- z2b | 1.08E+007 | 2.3 | 2.4 |
| 2e-4b | 4.73E+006 | 2.6 | 3.6 |
| 2f-2e | 2.75E+007 | 1.9 | 2.5 |
| 2f- z2 | 3.48E+006 | 2.7 | 2.5 |
| 2f- z2 | 7.65E+006 | 2.4 | 3.7 |
| 3f- x3 | 3.39E+007 | 1.9 | 4.7 |
| 3d-x2 | 1.40E+007 | 2.2 | 7.2 |
| 3f-3b | 1.02E+007 | 2.3 | 4.3 |
| 3f-3d | 9.54E+006 | 2.3 | 4.3 |
| 3f- x3 | 3.94E+006 | 2.7 | 2.4 |
| 4b-4f | 1.49E+007 | 2.2 | 4.3 |
| 4f- x5 | 1.14E+007 | 2.3 | 3.4 |

| | | | |
|---|---|---|---|
| 4b-2c | 1.42E+007 | 2.2 | 2.9 |
| 5b- w6 | 1.10E+007 | 2.3 | 4.8 |
| 5b- x5 | 5.80E+007 | 1.7 | 2.3 |
| 5b- x6 | 2.92E+007 | 1.9 | 2.7 |
| 5b- x7 | 6.41E+006 | 2.5 | 3.7 |
| 5b- z6 | 6.81E+006 | 2.5 | 5 |
| 6b-5b | 4.31E+006 | 2.6 | 4.6 |
| 6b-6c | 2.90E+007 | 1.9 | 2.5 |
| 6b-x5 | 6.40E+006 | 2.5 | 3.7 |
| 6b-x6 | 8.40E+006 | 2.4 | 2.6 |
| 6b-z6 | 2.81E+007 | 1.9 | 2.5 |
| 6c-4f | 9.07E+006 | 2.3 | 3.6 |
| 6e-4f | 5.31E+006 | 2.6 | 3.3 |
| 6f-6e | 4.26E+007 | 1.8 | 2.5 |
| 6f-OH(z6) | 8.86E+006 | 2.3 | 3.3 |
| 6f-w6 | 1.16E+007 | 2.2 | 2.8 |
| 6f-z6 | 3.65E+006 | 2.7 | 3.7 |
| 7f-Me | 1.51E+007 | 2.1 | 3.4 |
| 7f-x7 | 6.55E+006 | 2.5 | 3.6 |
| w5-4f | 1.64E+007 | 2.1 | 2.7 |
| w5-5f | 1.15E+007 | 2.2 | 2.9 |
| w5-x4 | 4.46E+007 | 1.8 | 2.3 |
| w5-x5 | 8.44E+006 | 2.4 | 2.9 |
| w7-5b | 3.64E+007 | 1.9 | 2.2 |
| w7-6b | 4.15E+006 | 2.7 | 4.1 |
| w7-7f | 4.32E+006 | 2.6 | 3.6 |
| w7-x5 | 9.98E+006 | 2.3 | 3.6 |
| w7-x6 | 1.90E+007 | 2.1 | 2.3 |
| w7-x7 | 1.71E+007 | 2.1 | 2.9 |
| w7-z6 | 1.63E+007 | 2.1 | 3.5 |
| x2-z2 | 1.37E+007 | 2.2 | 2.4 |
| x2-z2 | 8.81E+006 | 2.4 | 2.3 |
| x5-x6 | 4.00E+007 | 1.8 | 2.1 |
| x7-Me | 3.56E+006 | 2.7 | 4.2 |
| z2a-z2b (ref) | 4.38E+007 | 1.8 | 1.8 |
| z6-x5 | 8.88E+006 | 2.3 | 4.5 |
| z6-x6 | 2.12E+007 | 2.0 | 2.5 |

# A few atoms make the difference: synthetic, CD, NMR and computational studies on antiviral and antibacterial activities of glycopeptide antibiotic aglycon derivatives

Ilona Bereczki,[a] Attila Mándi,[b*] Erzsébet Rőth,[a] Anikó Borbás,[a] Ádám Fizil,[b] István Komáromi,[c] Attila Sipos,[a] Tibor Kurtán,[b] Gyula Batta,[b*] Eszter Ostorházi,[d] Ferenc Rozgonyi,[d] Evelien Vanderlinden,[e] Lieve Naesens,[e*] Ferenc Sztaricskai,[a] Pál Herczegh[a*]

[a]Department of Pharmaceutical Chemistry, Medical and Health Science Center, University of Debrecen, Egyetem tér 1, H-4010 Debrecen, Hungary,
[b]Department of Organic Chemistry, University of Debrecen, Egyetem tér 1, H-4010 Debrecen, Hungary,
[c]Vascular Biology, Thrombosis and Hemostasis Research Group, Hungarian Academy of Sciences, University of Debrecen, Nagyerdei krt. 98, H-4032 Debrecen, Hungary,
[d]Microbiology Laboratory, Department of Dermatology, Venerology and Dermatooncology, Semmelweis University, Mária u. 41, H-1085 Budapest, Hungary,
[e]Rega Institute for Medical Research, KU Leuven, B-3000 Leuven, Belgium

# Supporting Information

## Antiviral assays

The detailed procedure to evaluate the compounds for anti-influenza virus activity in Madin Darby canine kidney (MDCK) cells, can be found elswehere.[1] In brief, serial dilutions of the compounds were added to 96-well plates containing subconfluent cultures of MDCK cells. At the same time, influenza virus [A/H1N1 (strain A/PR/8/34 or A/Virginia/ATCC3/2009); A/H3N2 (strain A/HK/7/87); or B (strain B/HK/5/72)] was added at a multiplicity of infection of 0.0004 plaque-forming units per cell. After 72 h incubation at 35°C, microscopic inspection was done to score the virus-induced cytopathic effect (CPE) and calculate the compounds' 50% effective concentration ($EC_{50}$) values. In parallel, the compounds' cytotoxicity was determined as the minimal cytotoxic concentration (MCC). Then, the colorimetric MTS cell viability assay (CellTiter 96® $AQ_{ueous}$ One Solution Cell Proliferation Assay from Promega, Madison, WI, USA) was performed to confirm the 50% antivirally effective concentrations and calculate the 50% cytotoxic concentrations ($CC_{50}$).

## Antibacterial study

The antibacterial activity was tested against a panel of Gram-positive bacteria using broth microdilution method as previously described.[2]

## Computational data

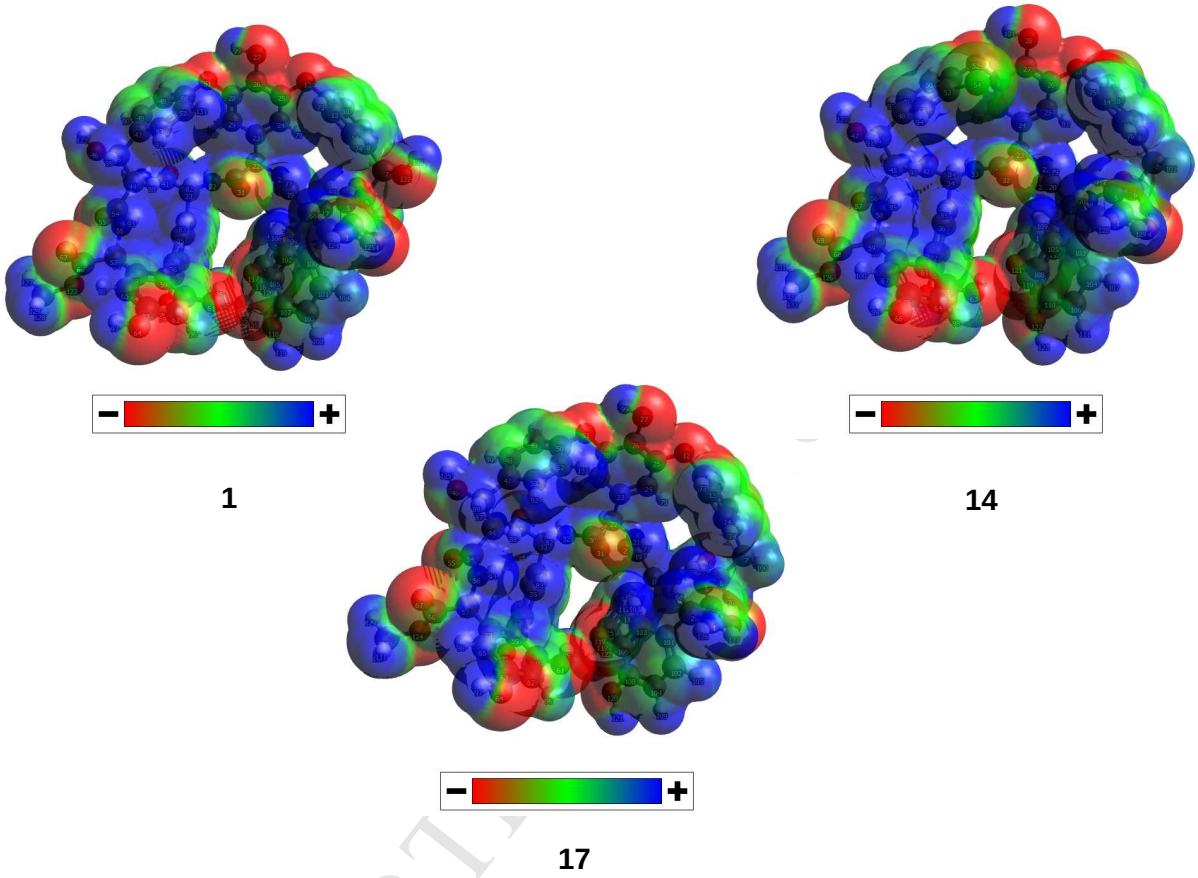


**Figure S1.** ESP (Merz–Kollman) charges computed for the B3LYP/6-31G reoptimized lowest-energy GAFF conformers of the three aglycons at HF/6-31G(d) level

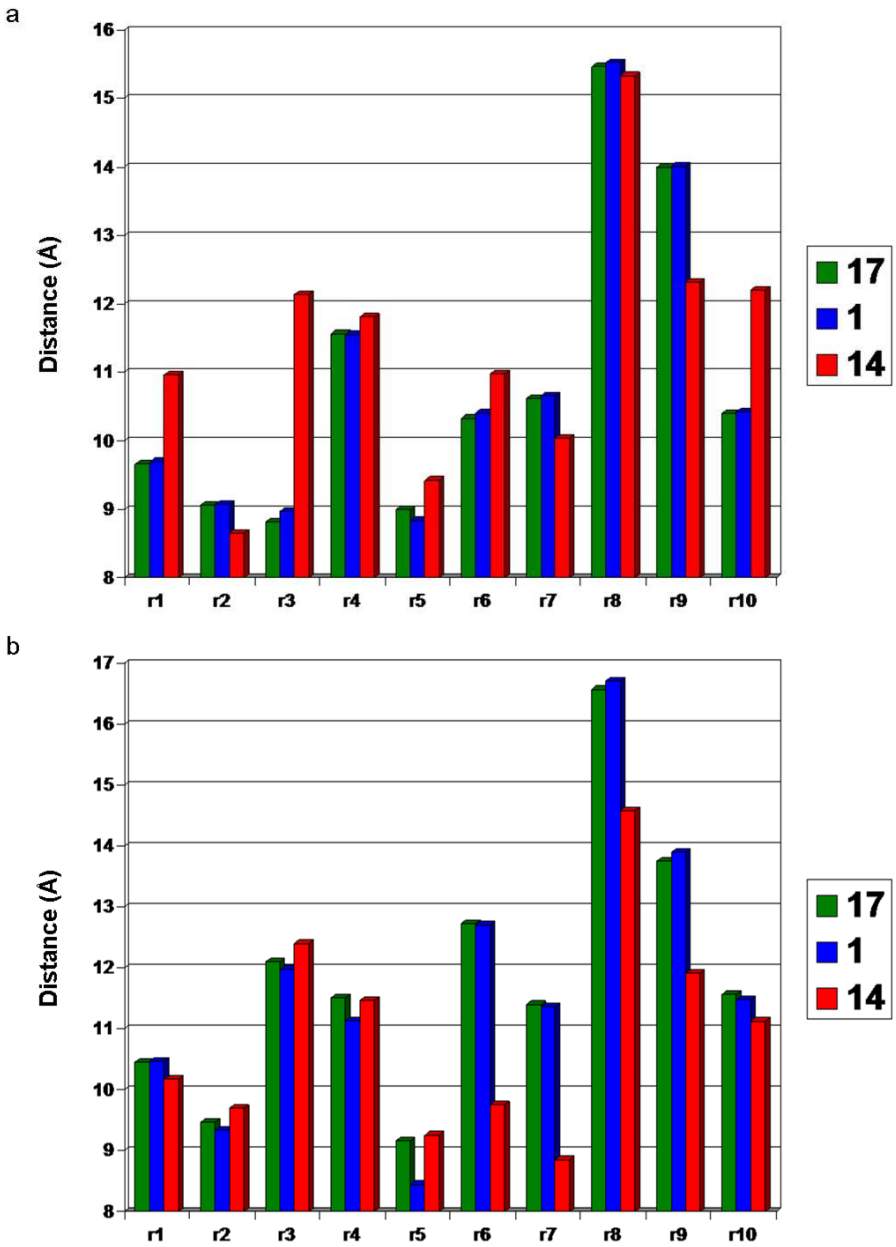


**Figure S2.** Comparison of some arbitrarily chosen characteristic distances of the a) lowest-energy conformers and b) equally weighted average of all low-energy conformers, optimized at GAFF level (r1 = 4d-***O***H – y6=***O*** , r2 = 4d-***O***H – x1-***N***$H_2$ , r3 = ***4d*** – x7-COO***C***$H_3$ , r4 = ***4d*** – 3e-***O***H , r5 = ***4d*** – 1d-***O***H , r6 = ***6d*** – 7e-***O***H , r7 = ***6d*** – 7c-***O***H , r8 = ***2d*** – 7e-***O***H , r9 = ***2d*** – 7c-***O***H, r10 = ***4d*** – 5d-***O***H)

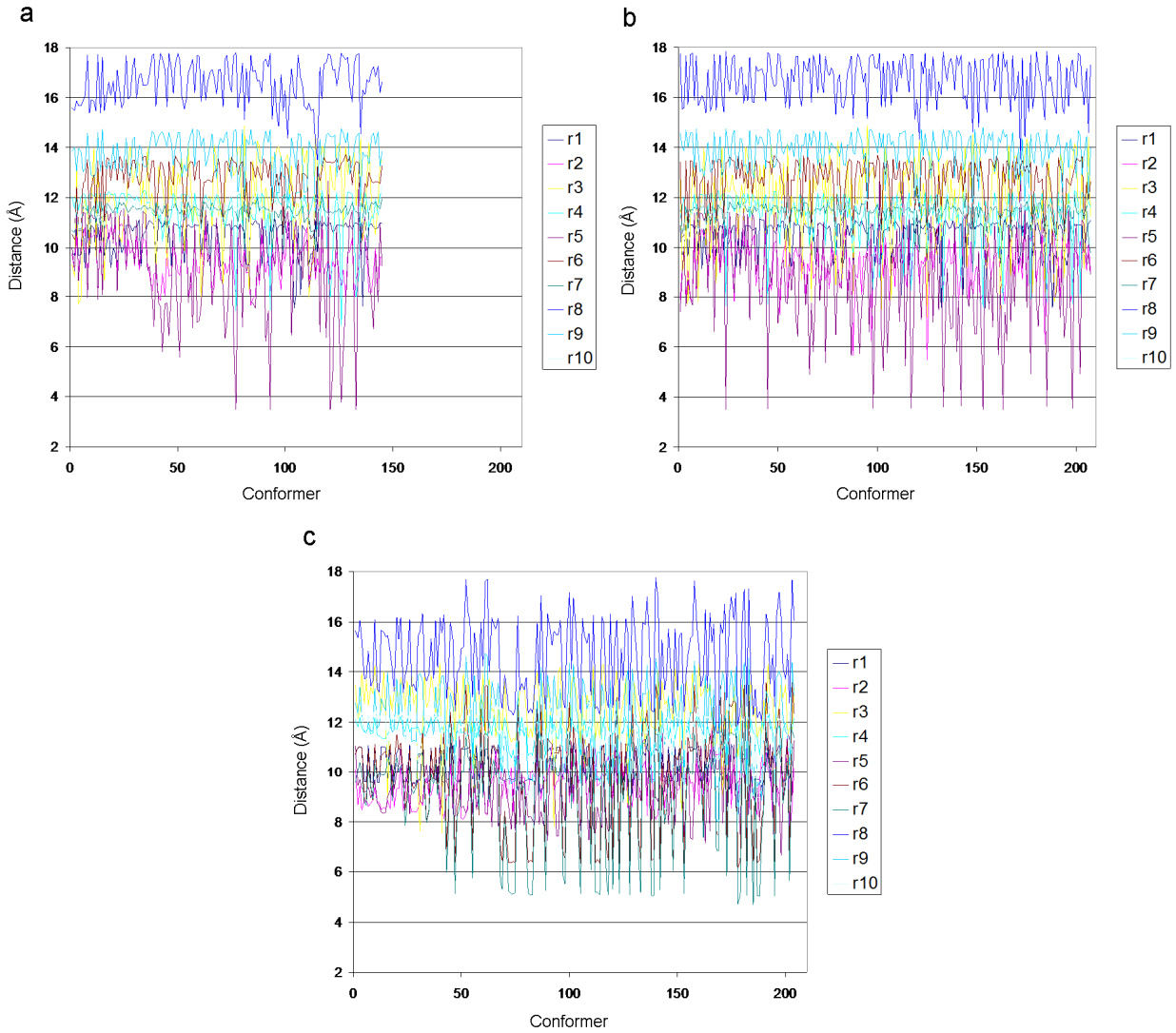


**Figure S3.** Comparison of some arbitrarily chosen characteristic distances of all low-energy conformers of the three aglycons optimized at GAFF level, a) **17**, b) **1** and c) **14** (r1 = 4d-***O***H – y6=***O*** , r2 = 4d-***O***H – x1-***N***$H_2$ , r3 = ***4d*** – x7-COO***C***$H_3$ , r4 = ***4d*** – 3e-***O***H , r5 = ***4d*** – 1d-***O***H , r6 = ***6d*** – 7e-***O***H , r7 = ***6d*** – 7c-***O***H , r8 = ***2d*** – 7e-***O***H , r9 = ***2d*** – 7c-***O***H, r10 = ***4d*** – 5d-***O***H).

## ECD spectra

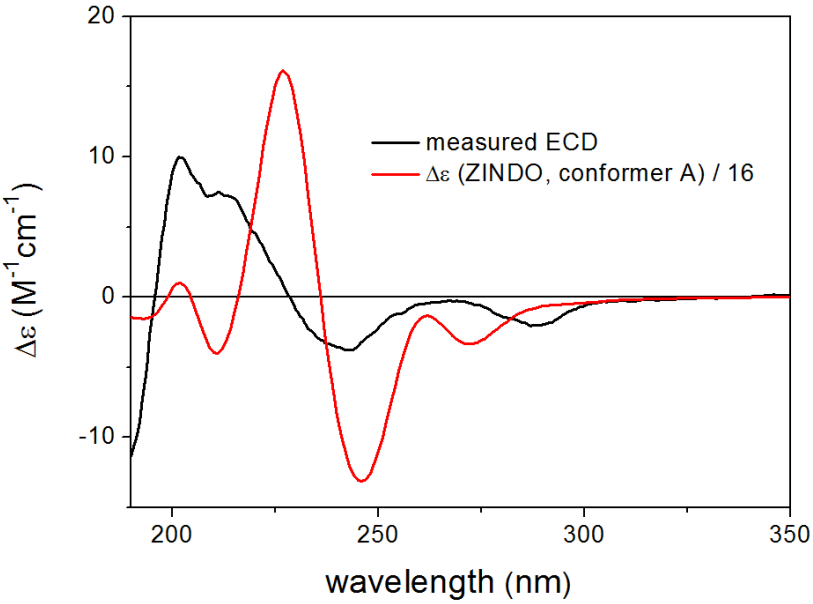


**Figure S4**. Experimental solution ECD spectrum (black) of **1** compared with the ZINDO-calculated ECD spectrum (red) for the lowest-energy B3LYP/6-31G PCM/$H_2O$ conformer of **1**

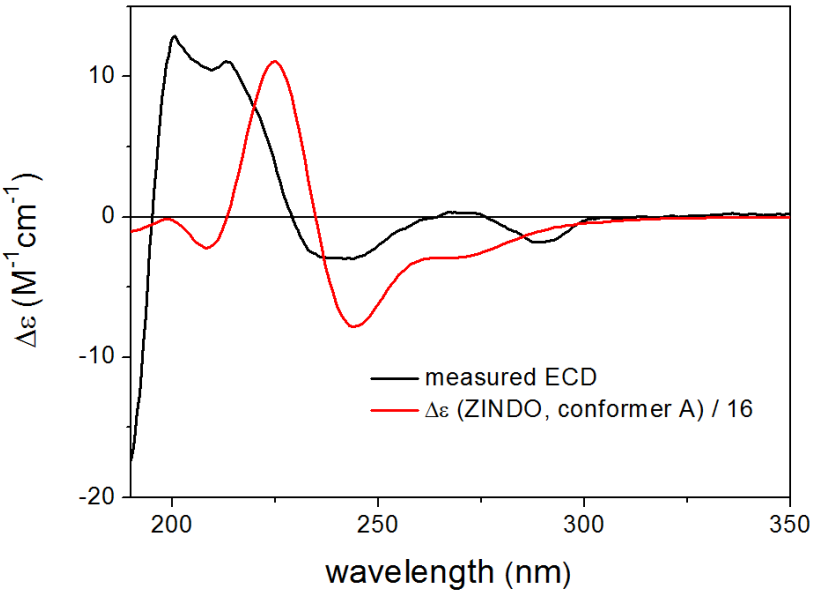


**Figure S5**. Experimental solution ECD spectrum (black) of **17** compared with the ZINDO-calculated ECD spectrum (red) for the lowest-energy B3LYP/6-31G PCM/$H_2O$ conformer of **17**

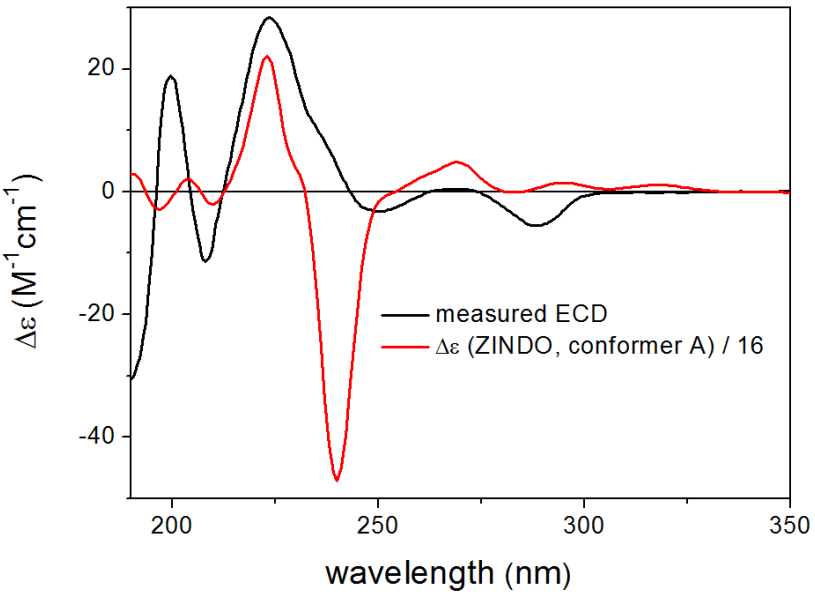


**Figure S6**. Experimental solution ECD spectrum (black) of 14 compared with the ZINDO-calculated ECD spectrum (red) for the 14-F model of the lowest-energy B3LYP/6-31G PCM/$H_2O$ conformer of **14**; half-height width = 900 $cm^{-1}$

## NMR spectra

HSQC spectrum of **1**

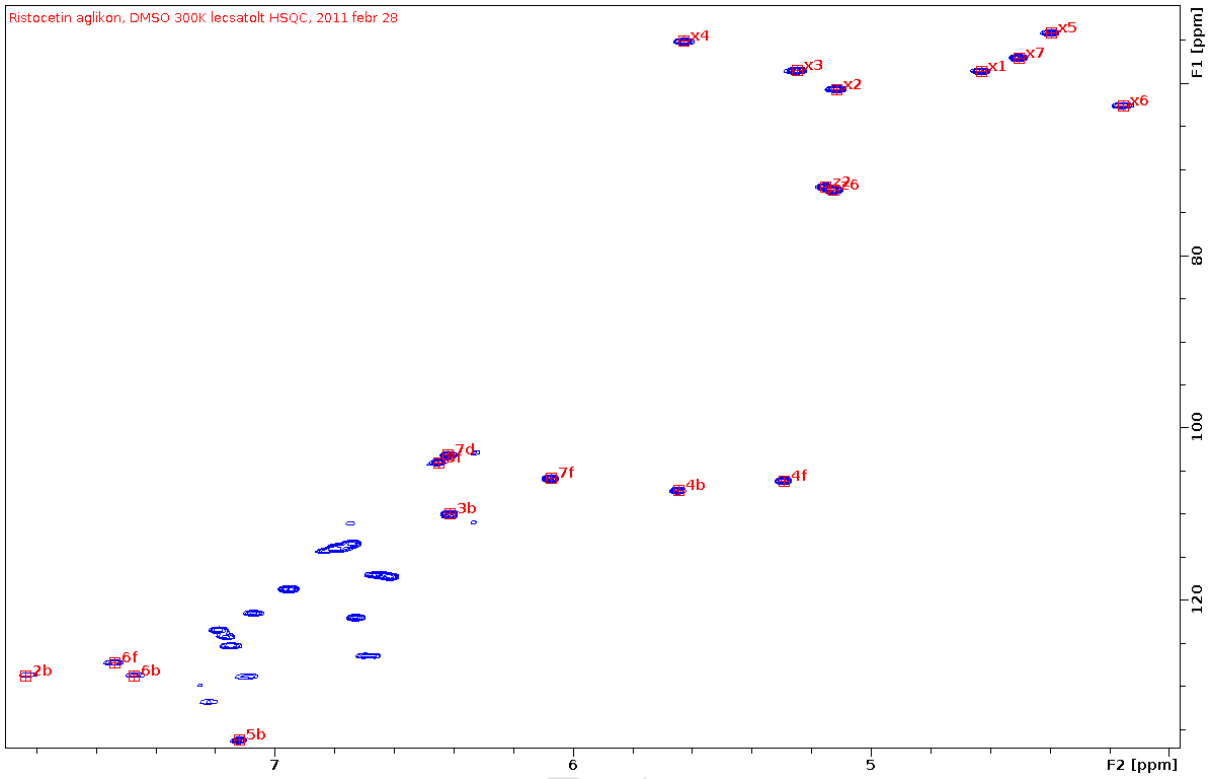

NMR spectra of **8** (13C, HSQC)

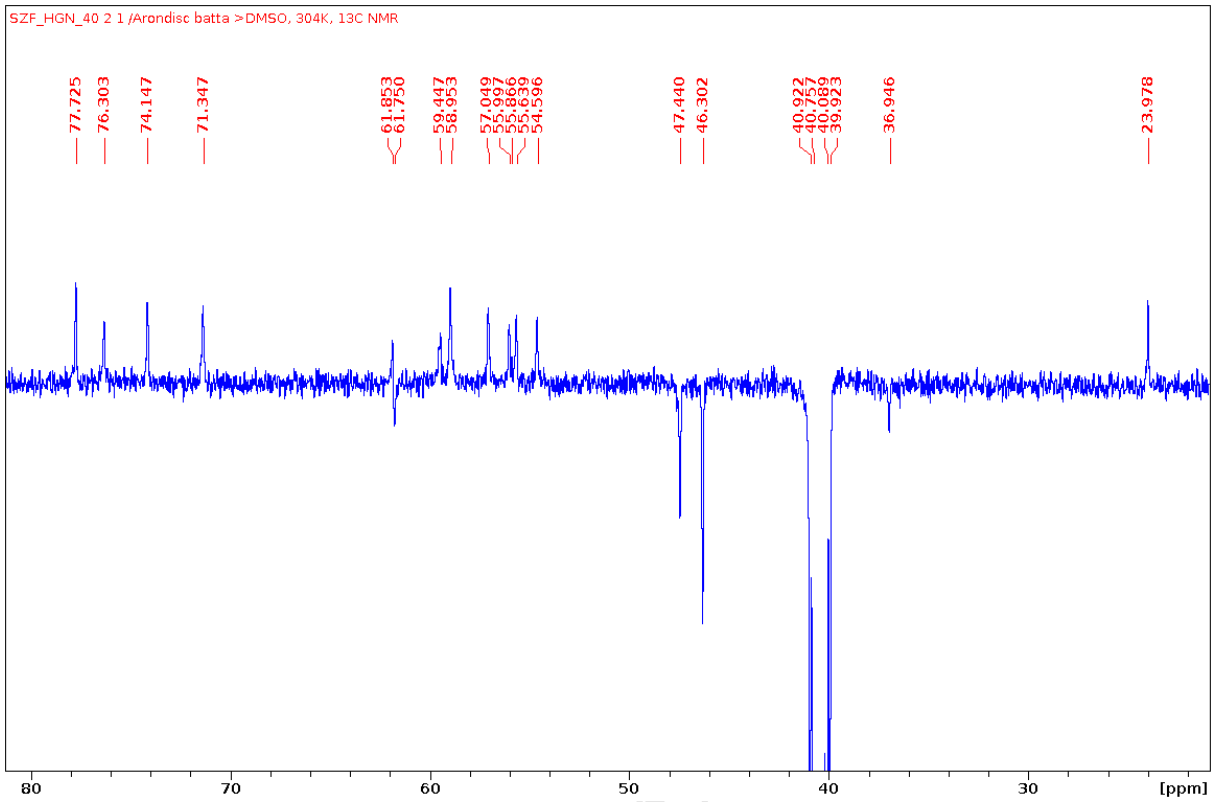


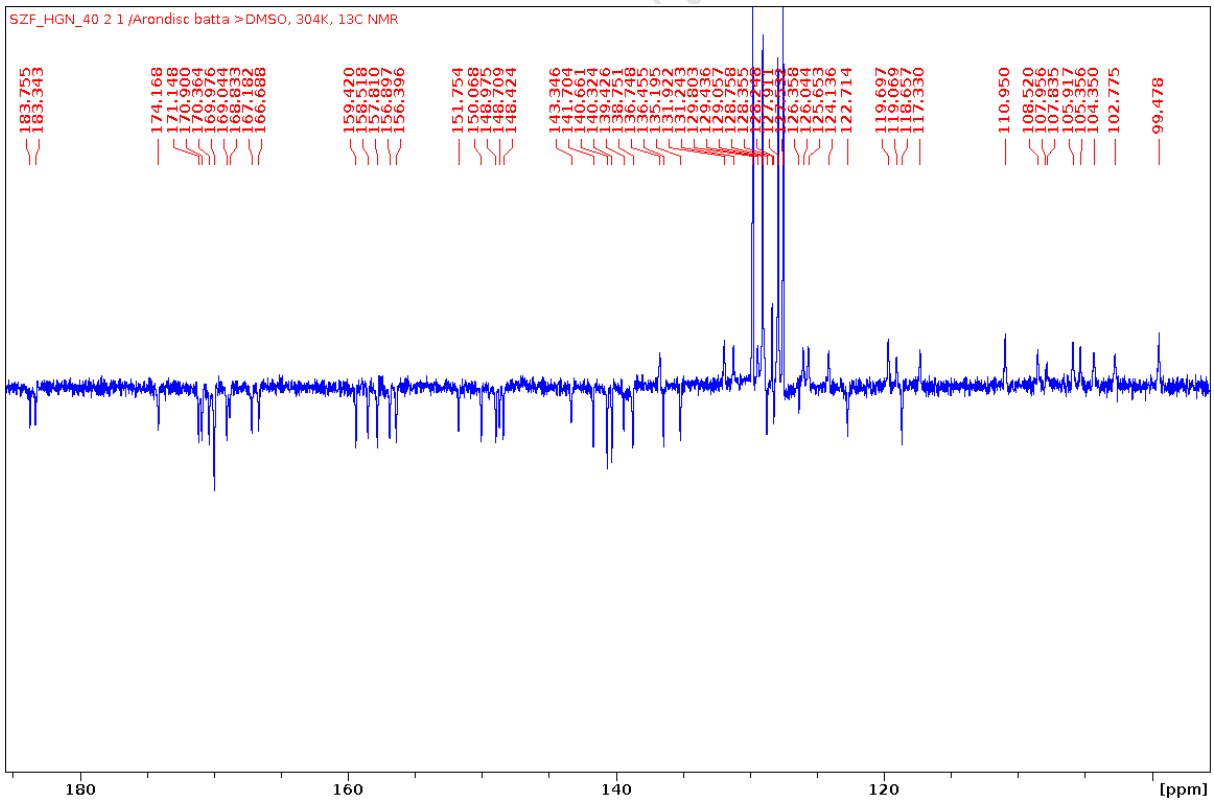

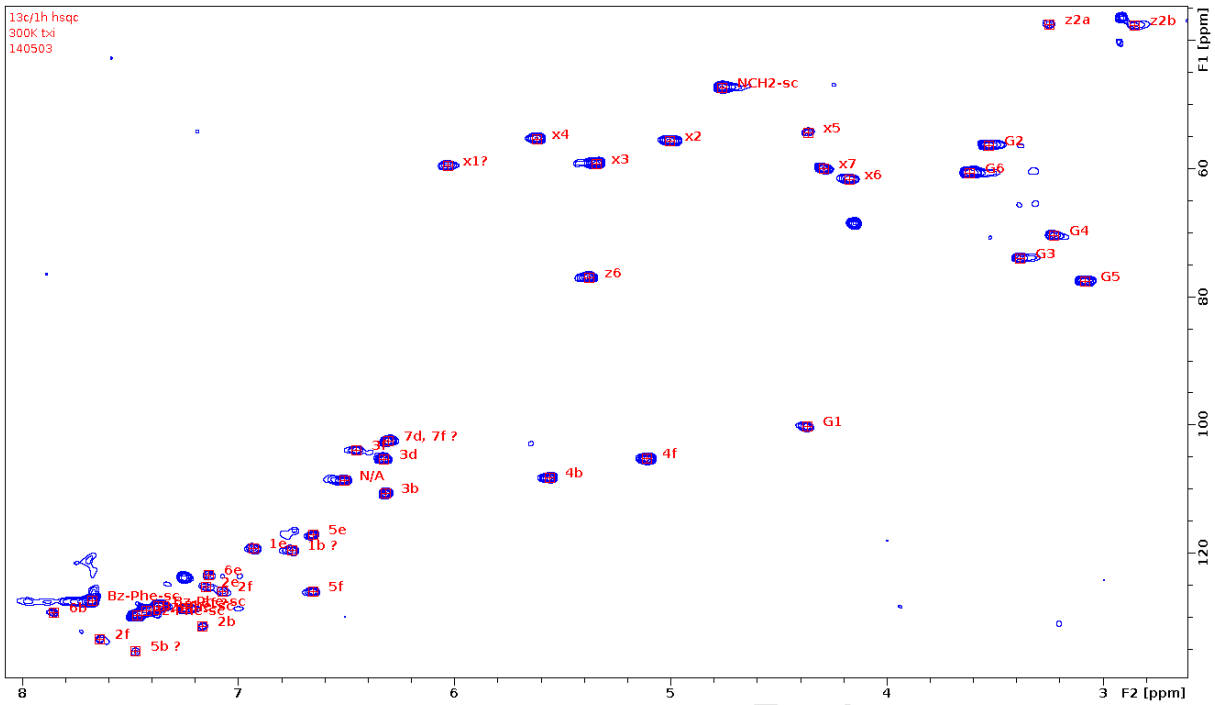


NMR spectra of **14** (13C, HSQC)

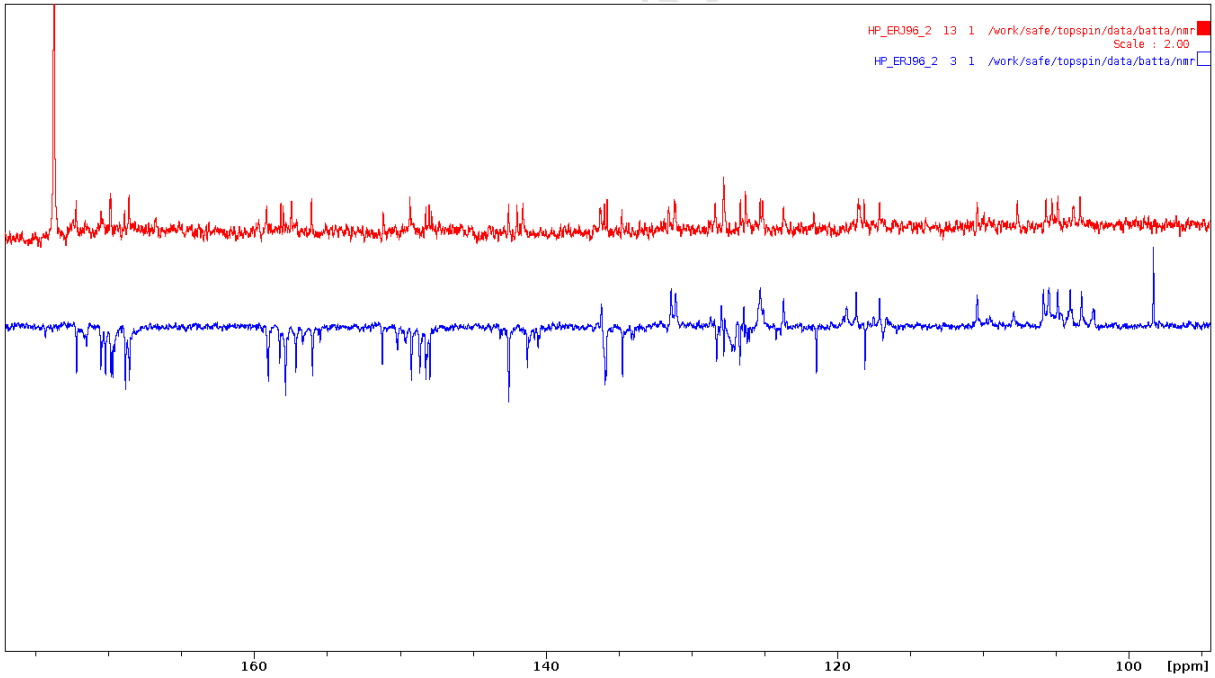

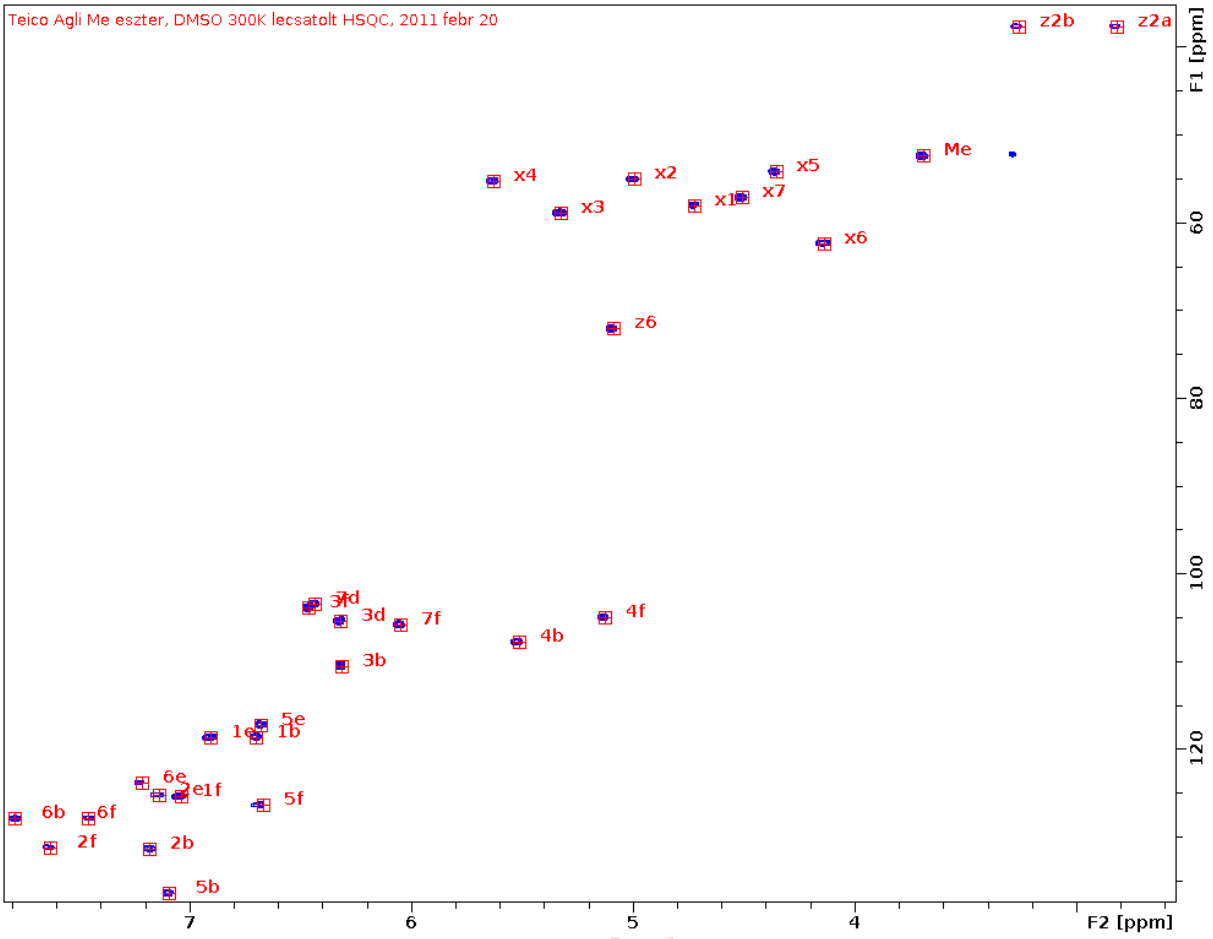


NMR spectra of **17** (HSQC)

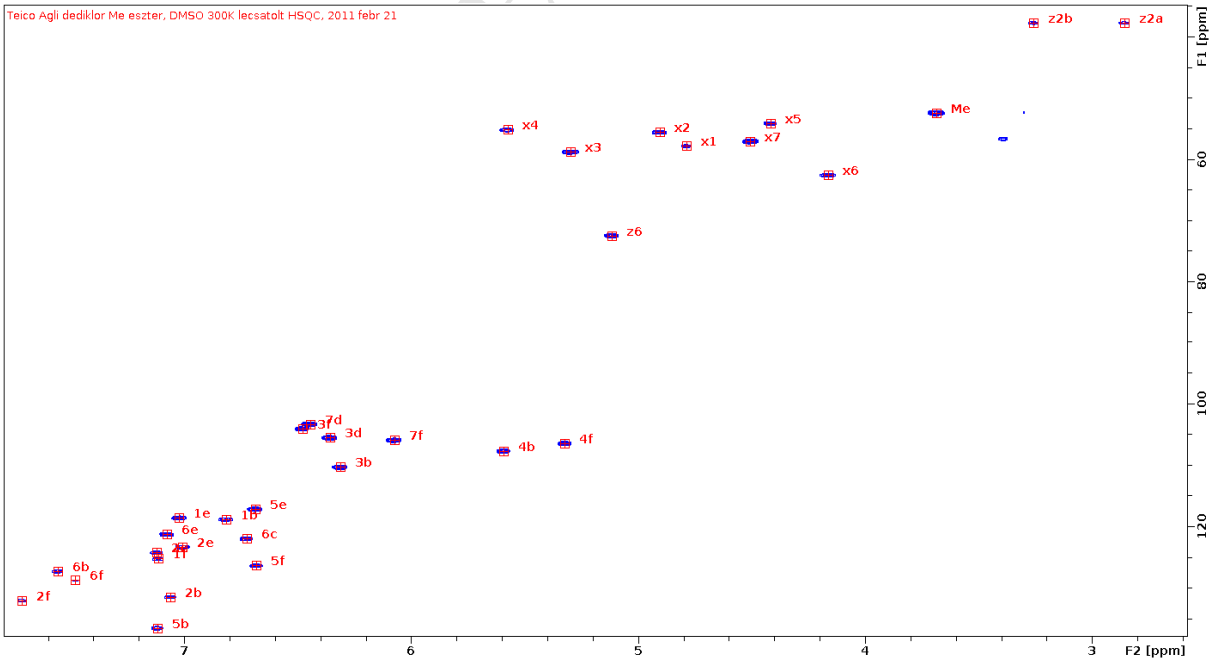

## References

1. Vanderlinden, E.; Vanstreels, E.; Boons, E.; ter Veer, W.; Huckriede, A;, Daelemans, D.; Van Lommel, A.; Rőth, E.; Sztaricskai, F.; Herczegh, P.; Naesens,L. Intracytoplasmic trapping of influenza virus by a lipophilic derivative of aglycoristocetin. *J. Virol.* **2012**, *86*, 9416-9431.
2. Sztaricskai, F.; Batta, G., Herczegh, P.; Balázs, A.; Jekő, J.; Rőth, E.; Szabó, P. T.; Kardos, S.; Rozgonyi, F.; Boda, Z. A new series of glycopeptide antibiotics incorporating a squaric acid moiety. *J. Antibiot*. **2006**, *59*, 564-582.

Highlights:

- Ristocetin and teicoplanin aglycon derivatives were prepared.
- Their antibacterial and anti-influenza virus activity was measured.
- The lipophilic side chain was crucial for the antiviral activity
- The effect of conformation on the antimicrobial activity was studied.
- Conformation-controlling effect of chloro substituents was identified.